Human Reproduction, Vol.29, No.12 pp. 2719–2735, 2014
Advanced Access publication on September 30, 2014 doi:10.1093/humrep/deu235

human reproduction **ORIGINAL ARTICLE** ***Reproductive biology***

Damaging legacy: maternal cigarette smoking has long-term consequences for male offspring fertility

A.P. Sobinoff[1,2], J.M. Sutherland[1,2], E.L. Beckett[3], S.J. Stanger[1,2], R. Johnson[3], A.G. Jarnicki[3], A. McCluskey[2], J.C. St John[4], P.M. Hansbro[3], and E.A. McLaughlin[1,2,5,*]

[1]Reproductive Science Group, School of Environmental & Life Sciences, University of Newcastle, Callaghan, NSW 2308, Australia [2]Priority Research Centre for Chemical Biology, University of Newcastle, Callaghan, NSW 2308, Australia [3]Centre for Asthma and Respiratory Disease, University of Newcastle and Hunter Medical Research Institute, Newcastle, Callaghan, NSW 2308, Australia [4]Centre for Genetic Diseases, MIMR-PHI Institute of Medical Research, Monash University, 27-31 Wright Street, Clayton Vic 3168, Australia [5]Monash Medical Centre, Monash Institute of Medical Research, Clayton, VIC 3168, Australia

*Correspondence address. PRC in Chemical Biology, School of Environmental & Life Sciences, University of Newcastle, Callaghan, NSW 2308, Australia. Tel: +61-2-4921-5708; Fax: +61-2-4921-6308; E-mail: eileen.mclaughlin@newcastle.edu.au

Submitted on May 4, 2014; resubmitted on August 20, 2014; accepted on August 25, 2014

STUDY QUESTION: What are the effects on fertility of cigarette smoke-induced toxicity on male offspring exposed during the gestational/weaning period?

SUMMARY ANSWER: Maternal cigarette smoke exposure during the gestational/weaning period causes long-term defects in male offspring fertility.

WHAT IS KNOWN ALREADY: Cigarette smoke is a well-known reproductive toxicant which is particularly harmful to both fetal and neonatal germ cells. However, recent studies suggest a significant portion of young mothers in the developed world still smoke during pregnancy. In the context of male reproductive health, our understanding of the effects of *in utero* exposure on offspring fertility is limited.

STUDY DESIGN, SIZE, DURATION: In this study, 27 C57BL/6 5-week-old female mice were exposed via the nose-only to cigarette smoke (treatment) or 27 were exposed to room air (control) for 6 weeks before being housed with stud males to produce litters. In the treatment group, smoke exposure continued throughout mating, pregnancy and lactation until weaning of pups at 21 days post birth. Male offspring were examined at post-natal days 3, 6, 12, 21 and 98 (adult).

PARTICIPANTS/MATERIALS, SETTING, METHODS: Approximately 108 maternal smoke-exposed C57BL/6 offspring and controls were examined. Spermatogenesis was examined using testicular histology and apoptosis/DNA damage was assessed using caspase immunohistochemistry and TUNEL. Sertoli cell morphology and fluctuations in the spermatogonial stem cell population were also examined using immunohistochemistry. Microarray and QPCR analysis were performed on adult testes to examine specific long-term transcriptomic alteration as a consequence of maternal smoke exposure. Sperm counts and motility, zona/oolemma binding assays, COMET analysis and mitochondrial genomic sequencing were also performed on spermatozoa obtained from adult treated and control mice. Fertility trials using exposed adult male offspring were also performed.

MAIN RESULTS AND THE ROLE OF CHANCE: Maternal cigarette smoke exposure caused increased gonocyte and meiotic spermatocyte apoptosis ($P < 0.01$) as well as germ cell depletion in the seminiferous tubules of neonatal and juvenile offspring. Aberrant testicular development characterized by abnormal Sertoli and germ cell organization, a depleted spermatogonial stem cell population ($P < 0.01$), atrophic seminiferous tubules and increased germ cell DNA damage ($P < 0.01$) persisted in adult offspring 11 weeks after exposure. Microarray analysis of adult offspring testes associated these defects with meiotic germ cell development, sex hormone metabolism, oxidative stress and Sertoli cell signalling. Next generation sequencing also revealed a high mitochondrial DNA mutational load in the testes of adult offspring ($P < 0.01$). Adult maternal smoke-exposed offspring also had reduced sperm counts with spermatozoa exhibiting morphological abnormalities ($P < 0.01$), affecting motility and fertilization potential. Odf2, a spermatozoa flagellum component required for coordinated ciliary beating, was also significantly down-regulated ($P < 0.01$) in maternal smoke-exposed adult offspring, with aberrant localization along the spermatozoa flagellum. Adult maternal smoke-exposed offspring took significantly longer to impregnate control females and had a slight but significant ($P < 0.01$) reduction in litter size.

LIMITATIONS, REASONS FOR CAUTION: This study examined only one species (mouse) using a smoking model which only simulates human cigarette smoke exposure.

WIDER IMPLICATIONS OF THE FINDINGS: This study represents the first comprehensive animal model of maternal smoking on male offspring reproductive function, suggesting that exposure during the gestational/weaning period causes long-term defects in male offspring fertility. This is due to a compromised spermatogonial stem cell population resulting from gonocyte apoptosis and impaired spermatogenic development. This results in significant germ cell damage and Sertoli cell dysfunction, impacting germ cell number, tubule organization, DNA damage and spermatozoa in adult offspring. This study strengthens the current literature suggesting that maternal exposure impairs male offspring fertility, which is currently debated due to conflicting studies.

STUDY FUNDING/COMPETING INTEREST(S): This study was funded by the Australian Research Council, Hunter Medical Research Institute, National Health and Medical Research Council of Australia and the Newcastle Permanent Building Society Charitable Trust. The authors declare no conflict of interest.

Key words: Cigarette smoking / subfertility / testis / DNA damage / spermatogenesis

Introduction

Maternal cigarette smoking during gestation is associated with a number of deleterious effects on offspring health, including premature delivery, fetal growth retardation and increased morbidity (Andres and Day, 2000; Habek *et al.*, 2002; Rogers, 2008). Despite an increased awareness of the adverse effects of maternal cigarette smoke exposure on offspring health, smoking prevalence among young women during pregnancy remains proportionally high, with ~20% of young women in the USA and ~36% of Australian mothers aged under 25 continuing to smoke during pregnancy (AIFS, 2011; CDC, 2011). In the context of male reproductive health, studies have observed reduced testes size and abnormal sperm counts and morphology in adult men exposed *in utero*, although these findings are not always consistent (Møller and Skakkebaek, 1997; Storgaard *et al.*, 2003; Belcheva *et al.*, 2004; Jensen *et al.*, 2004; Carmichael *et al.*, 2005; Damgaard *et al.*, 2008; Mamsen *et al.*, 2010). Indeed, a recent study by Fowler and colleagues did not detect any significant differences in testes size and weight, seminiferous tubule diameter or sex hormone levels in electively terminated second trimester male fetuses exposed *in utero*, although Sertoli cell desert hedgehog (*DHH*) signalling appeared to be perturbed (Fowler *et al.*, 2008). The ambiguity of these reports is confounded by a lack of controlled animal studies investigating the effects of maternal cigarette smoke exposure on male offspring reproductive health. Because linking reduced fertility and abnormal reproductive development with specific chemical exposures in humans is difficult due to uncontrolled conditions, the adverse effects of gestational maternal smoking on male offspring fertility remains poorly understood (Russell, 1991).

In this study we examined the effects of cigarette-induced reproductive toxicity on male offspring exposed during the gestational and weaning period using our novel inhalation exposure mouse model of cigarette smoke-induced chronic obstructive pulmonary disease and female subfertility (Beckett *et al.*, 2013; Sobinoff *et al.*, 2013). Our investigation focused on both the short- and long-term effects of exposure on spermatogenesis, seminiferous tubule morphology, sperm functionality and fertility in offspring.

Methods

Animals

All animal experimental procedures were performed with the approval of the University of Newcastle's Animal Care and Ethics Committee (ACEC). Specific pathogen-free adult female (5-week-old) C57BL/6 mice were obtained from the animal services unit and maintained according to the recommendations prescribed by the ACEC. Mice were housed under a controlled lighting regime (16L:8D) at 21–22°C and supplied with food and water *ad libitum*.

In utero smoke exposure

Cigarette smoke exposure was carried out as described previously (Beckett *et al.*, 2013). Briefly, C57BL/6 5-week-old female mice were exposed via the nose-only to cigarette smoke (twelve 3R4F reference cigarettes (University of Kentucky, USA) twice/day, five times per week, for 12–18 weeks). Each exposure lasted 60 min. Control mice received room air via the same apparatus. This level of exposure represents that of a 'pack a day' smoker (24 cigarettes/day), with the apparatus eliminating possible confounders caused by side-stream cigarette smoke exposure. In total, 27 mice underwent cigarette smoke exposure and the same number underwent the control treatment. Eleven-week-old female mice exposed or not to cigarette smoke for 6 weeks were separated into groups of three and housed with a single control stud male aged 7–8 weeks with proven fertility for a maximum of 12 weeks. Females were monitored every second day for post-coital plugs and pregnancy. Pregnant females were separated into single cages and litter sizes/pup weights recorded (Supplementary data, Fig S1) (Sobinoff *et al.*, 2013). Smoke exposure in the treatment group continued throughout mating, pregnancy and lactation until the weaning of pups at 21 days post birth.

Fertility trial

C57BL/6 8-week-old maternally exposed male mice ($n = 5$) were separated and housed with three control-virgin females aged 7–8 weeks for a maximum of 12 weeks. Females were monitored every second day for post-coital plugs and pregnancy. Pregnant females were separated into single cages and time to conception and litter sizes were recorded as described above.

Histological evaluation of testes

Testes were placed in Bouin's fixative for 24 h, washed in 70% ethanol, paraffin embedded and serially sectioned (4 μm thick) throughout half the testis, with every fourth slide counter-stained with haematoxylin and eosin (8–25 sections dependant on age). The number of seminiferous tubules per mm^2 was then counted on each haematoxylin and eosin section. Seminiferous tubule area for each tubule per section was then calculated using Image J software (NCBI), with results being normalized to control values. Pictures were taken using an Olympus DP70 microscope camera (Olympus America, Center Valley, PA, USA).

Immunohistochemistry

Testes for immunohistochemistry were fixed in Bouin's and sectioned 4 μm thick. Antibodies specific for Proliferating Cell Nuclear Antigen (PCNA, NA03T, Merck KGaA), active Casp2 (Casp2, ab2251, abcam), active Casp3 (Casp3, ab13847, abcam), tyrosine tubulin (T9028, SIGMA), Dmc1 (ab11054, abcam), PLZF (generously gifted by Dr Robin Hobb, Monash University) and SALL4 (ab29112, abcam) were used to probe testicular tissue sections using the following protocol. Slides were deparaffinised in xylene and rehydrated with subsequent washes in ethanol. Antigen retrieval was carried out by microwaving sections for 3 × 3 min in Tris buffer (50 mM, pH 10.6) or sodium citrate (10 mM, pH 6). Sections were then blocked in 3% BSA/TBS for 1.5 h at room temperature. The following solutions were diluted in TBS containing 1% BSA. Sections were incubated with either anti-PCNA (1:80), anti-Casp3 (1:200) or anti-tyrosine tubulin (1:200) for 1 h at room temperature. After washing in TBS containing 0.1% Triton X-100, sections were incubated with the appropriate fluorescent conjugated secondary antibodies (Alexa Fluor 594 goat anti-rabbit IgG, Alexa Fluor 594 goat anti-mouse IgG; 1:200 dilution) for 1 h. Slides were then counter-stained with 4′-6-Diamidino-2-phenylindole (DAPI) for 5 min, mounted in Mowiol and observed on an Axio Imager A1 fluorescent microscope (Carl Zeiss MicroImaging, Inc., Thornwood, NY, USA) under fluorescent optics and pictures were taken using a Olympus DP70 microscope camera (Olympus America). Experiments were performed in triplicate. Sections incubated with secondary antibody only following incubation with non-immune serum, from the animal in which the antibody was raised in, were used as controls for non-specific binding.

TUNEL analysis

Bouin's fixed sections were deparaffinised and rehydrated as mentioned previously. Sections were then boiled in Tris buffer (50 mM, pH 10.6) for 20 min and treated with 20 μg/ml Proteinase K for 15 min in a humidified chamber. TUNEL analysis was then performed using an In Situ Cell Death Detection Kit, Fluorescein (Roche Diagnostics Pty Ltd; Dee Why, NSW) according to the manufacturer's instructions. Slides were then counter-stained with DAPI for 5 min, mounted in Mowiol and observed using an Axio Imager A1 epifluorescent microscope (Carl Zeiss) and images were captured using an Olympus DP70 microscope camera (Olympus). Experiments were performed in triplicate.

RNA extraction

Total RNA was isolated from testes obtained from control and maternal smoke-exposed animals using two rounds of a modified acid guanidinium thiocyanate–phenol–chloroform protocol followed by isopropanol precipitation (Chomczynski and Sacchi, 1987; Sobinoff *et al.*, 2010).

Microarray analysis

Total RNA (~3 μg) was isolated from three control or maternal smoke-exposed adult testes using a QIAGEN RNeasy Mini Kit (Hilden, Germany) in accordance with the manufacturer's instructions. RNA was prepared for microarray analysis at the Australian Genome Research Facility (AGRF) using an Illumina Sentrix Mouse ref8v2 Beadchip. Labelling, hybridizing, washing and array scanning were performed by the AGRF using the Illumina manual on an Illumina BeadArray Reader, and normalized according to the quantile normalization method using GenomeStudio version 1.6.0 (Illumina, Inc., San Diego, CA, USA). All experiments were performed in triplicate with independently extracted RNAs. Statistically significant genes with more than a 1.4-fold difference in gene expression ($P < 0.05$ after False Discovery Rate adjustments), determined through the use of a 'volcano plot', were then analysed using Ingenuity Pathways Analysis (IPA, Ingenuity Systems, Redwood City, CA, USA) software to identify canonical signalling pathways influenced by cigarette smoke exposure. These values were selected based on the statistical consistency between biological replications and the smallest fold change required to observe an effect. The data discussed in this publication have been deposited in NCBI's Gene Expression Omnibus and are accessible through GEO Series accession number GSE51530 [http://www.ncbi.nlm.nih.gov/geo/query/acc.cgi?acc=GSE51530 (12 September 2014, date last accessed)].

Real-time PCR

Reverse transcription was performed with 2 μg of isolated RNA, 500 ng oligo(dT)15 primer, 40 U of RNasin, 0.5 mM dNTPs and 20 U of M-MLV-Reverse Transcriptase (Promega). Total RNA was DNase treated prior to reverse transcription to remove genomic DNA. Real-time PCR was performed using SyBr Green GoTaq qPCR master mix (Promega) according to manufacturer's instructions on an MJ Opticon 2 (MJ Research, Reno, NV, USA). Primer sequences along with annealing temperatures are supplied (Supplementary data, Table SI). Reactions were performed on cDNA equivalent to 100 ng of total RNA and carried out for 40 amplification cycles. SYBR® Green fluorescence was measured after the extension step at the end of each amplification cycle and quantified using Opticon Monitor Analysis software Version 2.02 (MJ Research). For each sample, a replicate omitting the reverse transcription step was undertaken as a negative control. Reverse transcription reactions were verified by β-actin PCR, performed for each sample in all reactions in triplicate. Real-time data were analysed using the equation $2^{-\Delta\Delta C(t)}$, where $C(t)$ is the cycle at which fluorescence was first detected above background fluorescence. Data were normalized to cyclophilin, and are presented as the average of each replicate normalized to an average of the reference genes (±SEM).

DNA extraction

DNA was extracted from tissues using the DNeasy Blood & Tissue kit in the presence of RNase A (Qiagen, West Sussex, UK), following the manufacturer's recommendations.

Long PCR

Two overlapping fragments that each span half of the mitochondrial genome were generated by long PCR amplification as templates for next generation sequencing. Reactions comprised 50 ng total DNA, 1× High Fidelity PCR buffer, 100 mM $MgSO_4$, 1 mM dNTPs (Bioline, London, UK), 1 U of Platinum Taq High Fidelity (Invitrogen, Carlsbad, CA, USA) and 10 μM each of the forward and reverse primer. Reaction conditions were 94°C for 2 min, 35 cycles of 94°C for 15 sec, 63°C for 30 sec and 68°C for 8 min 45 sec. Products were purified using the QIAquick PCR purification kit (Qiagen).

Next generation sequencing using the Ion Torrent Personal Genome Machine (PGM)™

Purified pairs of amplicons produced from long PCR were combined at equal concentrations. Amplicon libraries were generated using the Ion Fragment Library Kit and Ion Xpress™ Template kit (Life Technologies). MtDNA was sheared using the Covaris Adaptive Focused Acoustics (AFA™) system. Fragments of ~200 bp were selected following electrophoretic separation with the E-gel system (Life Technologies). Product size and quality was assessed by the Agilent Bioanalyzer using the Agilent High Sensitivity DNA Kit (Agilent, Santa Clara, CA, USA). Each DNA library was barcoded using different ligation adaptors. Libraries were then pooled at equal concentrations and loaded onto 316 chips for sequencing. Sequence alignment to the reference genome was performed using the Ion Torrent Suite (v.2.2). Variant selection was performed using CLC Genomics Workbench (v7.0.3). Reads were filtered to exclude those of<15 bp and one nucleotide was trimmed from both ends of each read. All reads accepted into analysis had a Phred quality score of 15. For inclusion into the final alignment, a

mismatch cost of 2 and an insertion/deletion cost of 3 was set; reads had a minimum of 80% identity to the reference sequence; and duplicate reads were excluded. A minimum mutation threshold of 3% was set.

Sperm analysis

Sperm were collected from male mice by dissecting the cauda epididymides and squeezing out the dense sperm mass along the tube. The sperm from each epididymis were then allowed to disperse into 2 ml of M2 medium for 15 min at 37°C in 5% CO_2 in air. Sperm counts and motility were performed using a haemocytometer. Sperm were then methanol fixed on Poly-L-Lysine slides and stained using the Diff-Quick Stain Kit (BDH, Poole, UK) for morphological analysis under light microscopy. Spermatozoa were then counted and designated as having normal or abnormal head or tail morphology (≥200 for each epididymis). Acrosomal staining was performed as follows. Slides were permeabilised with 0.15% Triton-X for 45 min. They were then incubated with 100 μg/ml FITC-conjugated peanut agglutinin (FITC-PNA, Sigma) for 40 min at 4°C, washed twice in PBS, and then counter-stained with DAPI for 5 min at room temperature, washed twice more in PBS and then mounted in 10% Mowiol. Slides were observed on an Axio Imager A1 epifluorescent microscope (Carl Zeiss MicroImaging, Inc.) under fluorescent optics and pictures were taken using a Olympus DP70 microscope camera (Olympus America). All preparations for analysis of morphology were coded and scored blind.

Immunocytochemistry

Sperm for immunocytochemical analyses were air-dried and methanol fixed on Poly-L-Lysine slides. Sections were blocked in 3% BSA/PBS for 1.5 h at room temperature. Anti-outer dense fibre of sperm tails 2 primary antibody (Odf2, ab43840, abcam) was diluted 1:10 in PBS containing 1% BSA and incubated at 4°C overnight. After washing in PBS containing 0.1% Tween, sections were incubated for 1 h at room temperature with Alexa Fluor 594 goat anti-rabbit IgG diluted 1:200 in PBS containing 1% BSA. Slides were then counter-stained with YOYO®-1 Iodide (491?509) for 5 min, mounted in Mowiol and observed on an Axio Imager A1 fluorescent microscope (Carl Zeiss MicroImaging, Inc.) under fluorescent optics and pictures were taken using a Olympus DP70 microscope camera (Olympus America). Experiments were performed in triplicate.

Comet analysis

The Neutral Comet Assay was performed on spermatozoa obtained from adult male mice using the CometAssay® kit (Trevigen, Gaithersburg, MD, USA) according to the manufacturer's instructions. Cells were observed on an Axio Imager A1 epifluorescent microscope (Carl Zeiss MicroImaging Inc.) under fluorescent optics and pictures were taken using an Olympus DP70 microscope camera (Olympus America). Sperm heads were counted for the either the presence or absence of fragmentation, and Olive Tail Moment calculated using CometScore (TriTek Corp, Sumerduck, VA, USA). Experiments were performed in triplicate.

Sperm-oocyte binding assays

Control C57BL/6 adult female mice (6 weeks) were super ovulated via ip injection of 10 IU of Folligon (equine chorionic gonadotrophin; Intervet, Sydney, Australia) followed by ip administration of 10 IU of Chorulon (human chorionic gonadotrophin [hCG]; Intervet) 48 h later. Cumulus-intact oocytes were recovered 12–15 h after the final hCG injection by rupturing the oviductal ampullae of superovulated animals in M2 medium (Sigma-Aldrich). Adherent cumulus cells were then dispersed by treating the collected oocytes with 300 IU/ml hyaluronidase solution (Sigma-Aldrich) and washing twice in M2 medium under oil. The zona pellucida was then removed from oocytes used for sperm oolemma binding assays by brief treatment with low-pH (2.5) Acid Tyrode's solution (Sigma-Aldrich) and allowed to recover for at least 1 h at 37°C in an atmosphere of 5% CO_2 in air. Sperm were collected from control and maternal smoke-exposed adult male mice (14 weeks of age) by dissecting the cauda epididymides and squeezing out the dense sperm mass along the tube. The sperm were then allowed to disperse into 800 μl M2 medium, diluted to a final concentration of 2×10^5 sperm/ml in M2 medium and allowed to capacitate for 3 h at 37°C in 5% CO_2 in air. Following capacitation, zona-free oocytes were preloaded with DAPI for 15 min; 12–25 oocytes were then added to the sperm suspensions and co-incubated for 15 min at 37°C in 5% CO_2 in air. Using serial aspiration through a finely drawn pipette, unbound and loosely adhered spermatozoa were removed from oocytes. Oocytes were then mounted on slides, and the number of sperm bound to the oocyte membrane was counted using phase-contrast microscopy. Sperm-oocyte fusion was then assayed by counting the number of DAPI stained sperm heads attached to the oocyte membrane using fluorescent microscopy. Experiments were performed in triplicate.

Statistics

Comparisons between control and treatment groups were performed using one-way analysis of variance (ANOVA) and Student's *t*-test using the litter as the statistical unit. The assigned level of significance for all tests was $P < 0.05$.

Results

Maternal cigarette smoke exposure during the gestational/weaning period severally depletes testicular germ cells via apoptosis

Histological assessment of both control and maternal smoke-exposed (MSE) testes revealed gross morphological changes between both groups in neonatal offspring (Fig. 1), including the presence of atrophic seminiferous tubules in MSE offspring. PCNA, a marker of mitotic proliferation and DNA repair, was used to visualize gonocytes, spermatogonial and putative damaged germ cells within the seminiferous tubules of all smoke-exposed groups (Fig. 1A). Intensely fluorescent gonocytes, representative of DNA damage, were detected in PND3 smoke-exposed seminiferous tubules and absent in control animals. There was no observable difference in PCNA staining between control and MSE testes at PND6, but by PND12 MSE animals had an observable decrease in PCNA positive spermatogenic cells, with some seminiferous tubules being devoid of germ cells altogether. A significant increase ($P < 0.05$) in the number of seminiferous tubules/mm^2 (Fig. 1B) together with a significant decrease in seminiferous tubule area (Fig. 1C) was also observed in MSE neonatal testes, suggesting a decrease in germ cell content.

Germ cell markers ?h2ax and Pka were used to visualize intermediate spermatogonia, pachytene spermatocytes and round spermatids in both juvenile (PND 21) and adult MSE testes (Fig. 2A). Histomorphological analysis revealed that MSE juvenile testes contained disrupted seminiferous tubules with a partial or complete loss of germ cells, abnormal seminiferous tubule morphology (Fig. 2A), and decreased testicular weight (Supplementary data, Fig. S2) persisting into adulthood. Both juvenile and adult MSE testes had a small but significant increase ($P < 0.05$) in seminiferous tubules/mm^2 (Fig. 2B) and a significant decrease in seminiferous tubule area (Fig. 2C), indicating reduced germ cell content, although these differences were less severe in the adult.

Analysis of classical apoptosis markers showed increased cell death in smoke-exposed neonatal/juvenile testes compared with control animals. The early markers of apoptosis, activated Casp2 and Casp3,

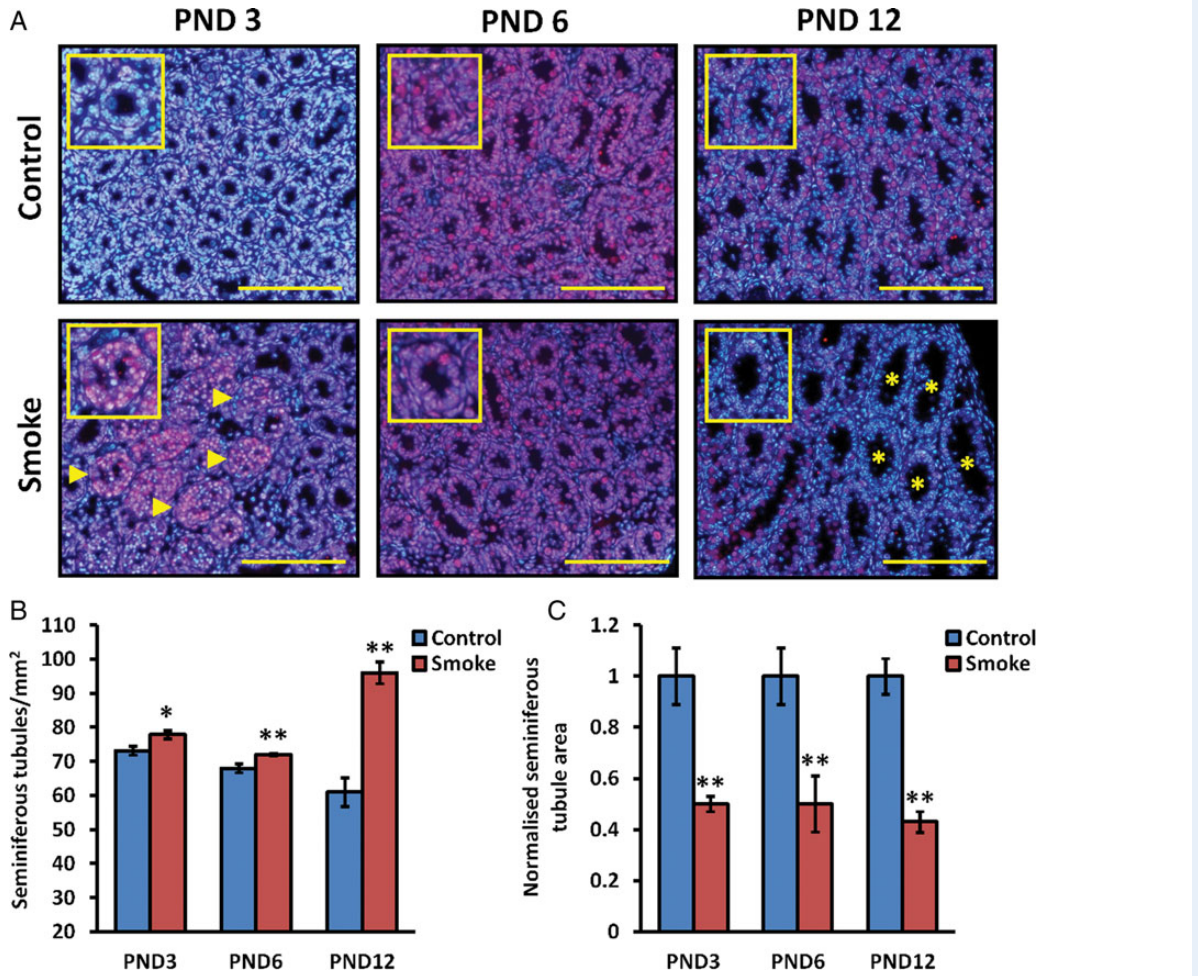

Figure 1 Maternal cigarette smoke exposure causes germ cell depletion in neonatal offspring. (**A**) Fluorescent PCNA (marker of proliferation and DNA repair) immunohistological staining visualized via epifluorescent microscopy. Images are representative of $n = 3$ experiments on $n = 3–5$ testes. Blue staining (DAPI) represents nuclear staining in all cells; red staining (Cy-5) represents specific staining for PCNA protein. Arrow head = intense PCNA fluorescence indicative of DNA damage highlighted in insert at higher magnification; Asterisk = tubules devoid of germ cells. Scale bar is equal to 100 μm. (**B**) Average number of seminiferous tubules counted per mm^2. Values are mean ± SEM, $n = 3–5$ testes from individual mice belonging to different litters. The symbols * and ** represent $P < 0.05$ and $P < 0.01$, respectively, in comparison with control values. (**C**) Average area of seminiferous tubules per treatment (mm^2). Results are normalized to control values. Values are mean ± SEM, $n = 3–5$ testes from individual mice belonging to different litters. The symbols * and ** represent $P < 0.05$ and $P < 0.01$, respectively, in comparison with control values.

were detected in PND3 and PND6 gonocytes, PND12 spermatogonia, and PND21 pachytene spermatocytes (Figs 3A and 4A). TUNEL staining, a technique used to detect DNA strand breaks and therefore end stage apoptosis, was also detected in germ cells at each neonatal/juvenile time point (Fig. 5A). Overall there was a significant increase ($P < 0.01$) in seminiferous tubules positive for Casp3 (~3–13-fold), Casp2 (~3–16-fold) and TUNEL (~3–10-fold) in MSE PND3, 12 and 21 testes (Figs 3B, 4B and 5B). With the exception of Casp3, PND6 MSE testes did not have a significant increase in apoptotic markers, suggesting decreased vulnerability to xenobiotic induced stress at this time point.

The spermatogonial stem cell markers SALL4 and PLZF were used to visualize spermatogonial stem cells in both control and smoke-treated animals (Fig. 6). Germ cells with positive staining for either stem cell marker were significantly reduced in MSE neonatal, juvenile and adult testes (Fig. 6).

The detection of apoptotic germ cells and depleted spermatogonia-specific stem cell markers, in addition to reduced seminiferous tubule diameter and abnormal morphology in neonatal/juvenile testes, suggests that the early stages of testicular development are vulnerable to maternal smoke exposure, impairing the establishment of the spermatogonial stem cell population and meiotic development.

Maternal cigarette smoke exposure causes recurring DNA damage in adult germ cells and abnormal Sertoli cell development

In order to examine the long-term effects of maternal smoke exposure on male germ cell development, we examined Casp2 and Casp3 expression in adult MSE testes. Both of these early markers of apoptosis were not present above control levels in smoke-exposed animals, suggesting

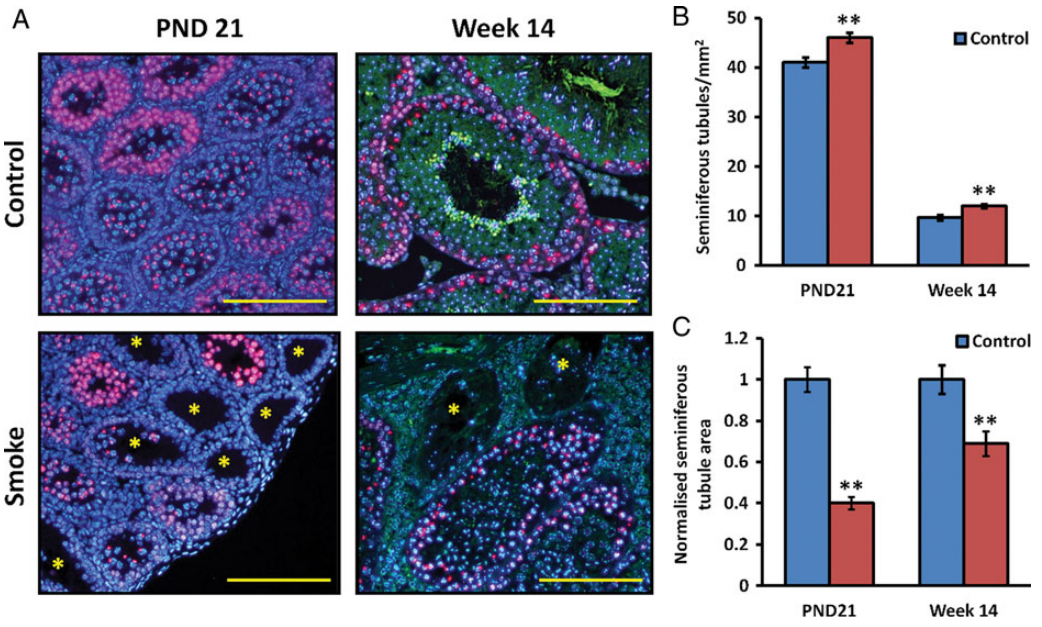

Figure 2 Maternal cigarette smoke exposure causes germ cell depletion in juvenile offspring, with depleted tubules persisting into adulthood in exposed offspring. (**A**) Fluorescent immunohistological staining visualized via epifluorescent microscopy. Images are representative of $n = 3$ experiments on $n = 3–4$ testes from individual mice belonging to different litters. Blue staining (DAPI) represents nuclear staining in all cells; red staining (Cy-5) represents specific staining for ?h2ax protein (marker of intermediate spermatogonia and pachytene spermatocytes); green staining (FITC) represents specific staining for Pka protein (marker of round spermatids). Asterisk = tubules devoid of germ cells. Scale bar is equal to 100 μm. (**B**) Average number of seminiferous tubules counted per mm^2. Values are mean ± SEM, $n = 3–4$ testes from individual mice belonging to different litters. The symbols * and ** represent $P < 0.05$ and $P < 0.01$ in comparison with control values, respectively. (**C**) Average area of seminiferous tubules per treatment (mm^2). Results are normalized to control values. Values are mean ± SEM, $n = 3–4$ testes from individual mice belonging to different litters. The symbol ** represents $P < 0.01$ in comparison with control values.

an absence of active apoptosis (Fig. 7). However, we observed an increase in the number of seminiferous tubules with germ cells positive for TUNEL staining; suggesting DNA damage was still being induced 11 weeks after maternal smoke exposure (Fig. 7B). As the identity of spermatogenic cells experiencing DNA damage was unclear from TUNEL staining alone, we assessed for the presence of markers of DNA damage repair preferentially expressed at different stages of spermatogenesis. Dmc1, a meiosis-specific homologue of Rad51 which repairs double strand breaks during meiosis, was assessed in pachytene spermatocytes (Fig. 8A). Intensely fluorescent spermatogenic cells were identified as being in a state of DNA repair, with the number of tubules containing three or more of these cells being scored in control and smoke-exposed animals. MSE animals had significantly more tubules with intensely fluorescent cells (~2-fold, $P < 0.01$), suggesting meiotic cell DNA repair. As described previously, PCNA is a marker of mitotic proliferation and DNA repair, and was used to observe DNA repair in spermatogonia (Fig. 8B). Like Dmc1, MSE animals had significantly more tubules with intensely fluorescent PCNA-positive cells (~3-fold, $P < 0.01$), suggesting mitotic cell DNA repair. Collectively, these results reveal a continuing legacy of DNA damage affecting both mitotic and meiotic spermatogenic cells in MSE animals.

Continued DNA damage in adult MSE germ cells led us to examine whether abnormal Sertoli cell development/function was contributing to the persistent testicular pathology (Supplementary data, Fig. S3). The Sertoli cell cytoplasm was visualized by tyrosine tubulin immunofluorescence (Fig. 9). A significant increase in the number of atrophic tubules containing Sertoli cells ($P < 0.01$) with increased vacuolization was observed in both PND21 and adult MSE animals. These results suggest that maternal smoke exposure causes Sertoli cell damage in juvenile offspring, with persistent testicular pathology in the adult, contributing to germ cell DNA damage.

Effects of maternal cigarette smoke exposure on testicular gene expression and cell signalling pathways in the adult

MSE caused a significant change in total testicular gene expression, with 108 genes being significantly ($P < 0.05$) altered in MES adult testes. Grouping according to their molecular and cellular function revealed a large proportion of these significantly altered genes were implicated in cancer (41%), small molecule biochemistry (36%), tissue development (20%), reproductive system development/function (19%) and reproductive system disease (19%) (Supplementary data, Table SII and SIV). Using IPA, the top canonical pathways which were significantly altered in maternally exposed adult offspring were also identified (Supplementary data, Fig. S4 and Table SIII). Maternal cigarette smoke exposure influenced genes in pathways involved in spermatogenesis (retinol metabolism, sex hormone metabolism and glycolipid metabolism),

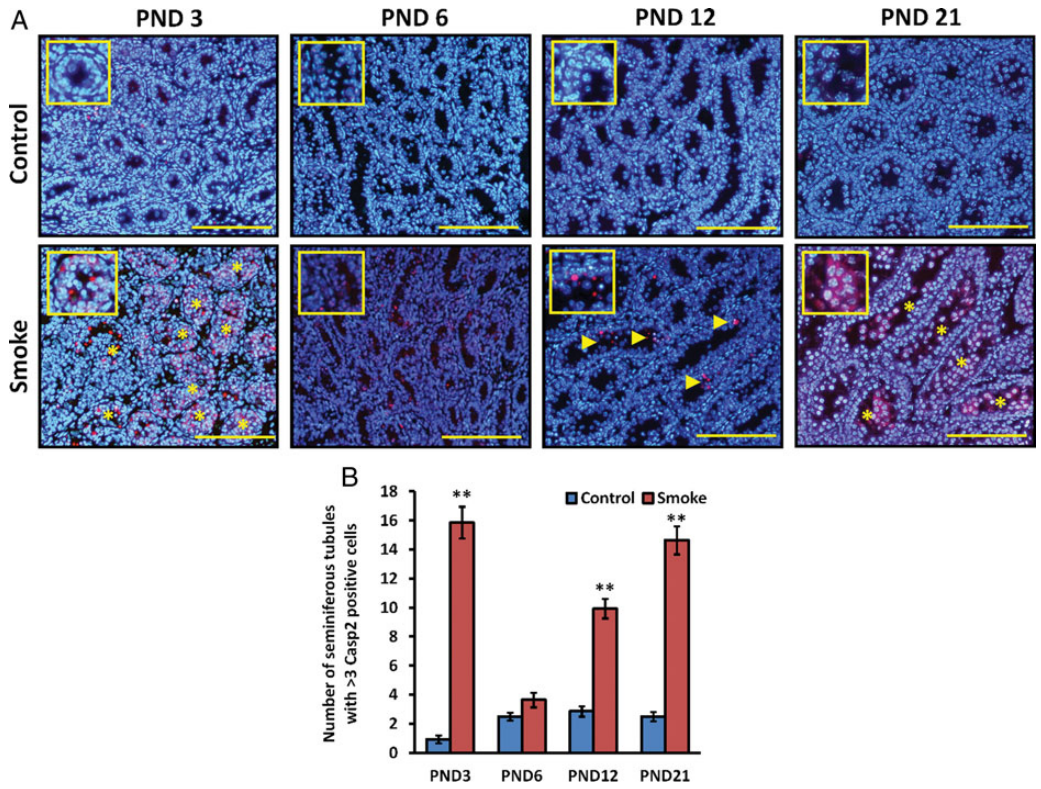

Figure 3 Maternal cigarette smoke exposure causes seminiferous tubule apoptosis in neonatal and juvenile offspring. (**A**) Fluorescent Casp2 (marker of apoptosis) immunohistological staining visualized via epifluorescent microscopy. Images are representative of $n = 3$ experiments on $n = 3–5$ testes from individual mice belonging to different litters ($n = 9–15$ sections). Blue staining (DAPI) represents nuclear staining in all cells; red staining (Cy-5) represents specific staining for Casp2 protein. Arrow head = intense Casp2 fluorescence indicative of DNA damage in individual cells highlighted in insert at higher magnification; Asterisk = tubules with extensive Casp2 staining. Scale bar is equal to 100 μm. (**B**) Quantification of the number of seminiferous tubules containing >3 Casp2 positive cells. Values are mean ± SEM, $n = 3$ experiments on $n = 3–5$ testes from individual mice belonging to different litters ($n = 9–15$ sections). The symbol ** represents $P < 0.01$ in comparison with control values.

detoxification (xenobiotic metabolism), oxidative stress (glutathione metabolism), energy production (glycolysis) and Sertoli cell function (tight junction signalling).

Validation of microarray results was performed via qPCR (Supplementary data, Table SV). Similar gene expression patterns were observed for all targets measured by qPCR compared with the microarray results. A number of genes which play important roles in spermiogenesis (*Ybx2*, *Acot7*, *Slc30a1* and *Sycp1*) or act as biomarkers of maturing spermatozoa (*Acap4* and *Odf2*), were down-regulated in MSE animals. Other validated genes involved in testosterone production (*Cyp17a1*, *Cyp11a1*), oxidative stress/retinol metabolism (*Retstat* and *Txnip*) and Sertoli cell function (*Timp2*) were confirmed to be up-regulated in MSE animals.

Effects of maternal cigarette smoke exposure on the integrity of the mitochondrial genome in testis and lung tissue

Given the increase in oxidative stress markers observed through microarray analysis, we examined the integrity of the mitochondrial genome in the testis and lungs of MSE animals using next generation sequencing. We identified 248 rearrangements in the mitochondrial genomes of testis and lung tissue from adult MSE mice (Supplementary data, Table SVI) when compared with control testes. Of these 248 rearrangements, 9 were single nucleotide variants (SNV) and 6 were insertions. The remainder were single nucleotide deletions. Of the rearrangements, 115 were specific to the testis whilst 56 were specific to the lung. This strongly suggests that the mitochondrial genomes of testicular cells including germ cells are more vulnerable to the effects of smoking than the lung.

In all, there were 90 rearrangements, which were present at over 5% in one or both of the tissues analysed (Supplementary data, Table SVII); 37 of the variants were present either exclusively or at >5% in the testis tissue. On the other hand, 24 of the variants were exclusively present or at >5% in the lung tissue. The reminding variants were present in both tissues at similar levels (i.e. <5% difference). The most prevalent variants (>15%) were at nt 642, 1070, 2471, 2511, 2610, 3727, 4274, 4504, 4509, 4889, 4925, 10818, 11275, 11890, 13199, 13481, 13893, 14213, 14936, 15160 and 15601. Of this cohort, 10 were specific to the testis only and 4 to the lung. The highest prevalence was at nt2471 (91.98%), nt2511 (51.72%) and nt10818 (41.98%). The variant at nt14213 was present at 74.14 and 69.92% in the testis and lung, respectively.

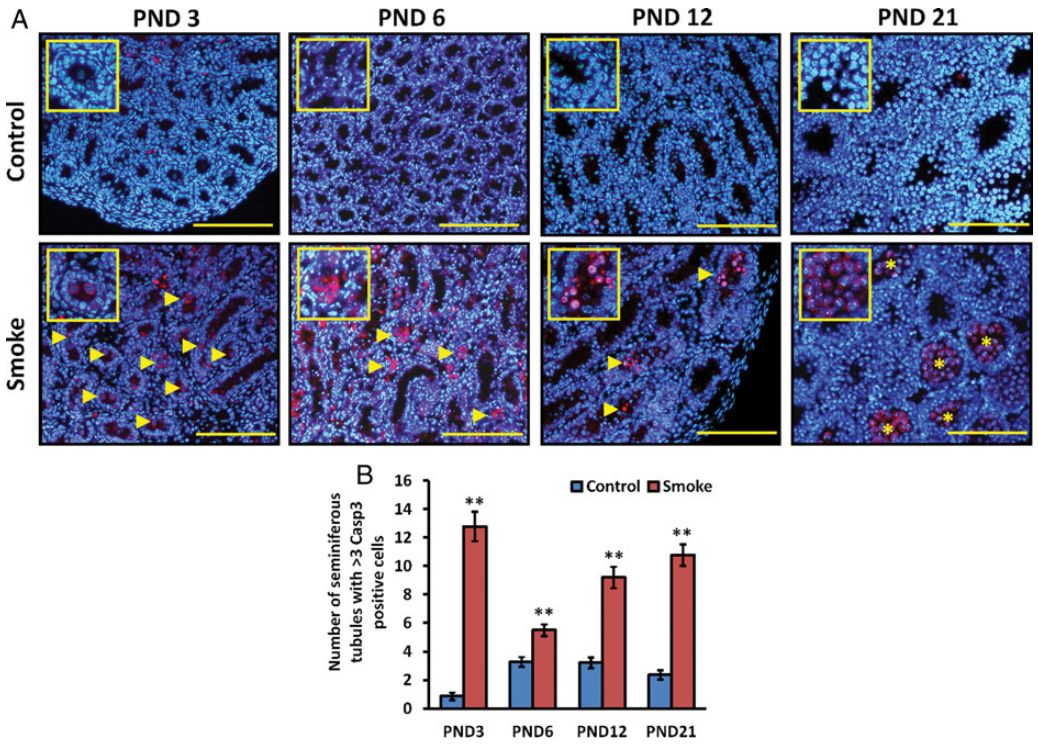

Figure 4 Maternal cigarette smoke exposure causes seminiferous tubule apoptosis in neonatal and juvenile offspring. (**A**) Fluorescent Casp3 (marker of apoptosis) immunohistological staining visualized via epifluorescent microscopy. Images are representative of $n = 3$ experiments on $n = 3–5$ testes from individual mice belonging to different litters ($n = 9–15$ sections). Blue staining (DAPI) represents nuclear staining in all cells; red staining (Cy-5) represents specific staining for Casp3 protein. Arrow head = intense Casp3 fluorescence indicative of DNA damage in individual cells highlighted in insert at higher magnification; Asterisk = tubules with catastrophic Casp3 staining. Scale bar is equal to 100 μm. (**B**) Quantification of the number of seminiferous tubules containing >3 Casp3 positive cells. Values are mean ± SEM, $n = 3$ experiments on $n = 3–5$ testes from individual mice belonging to different litters ($n = 9–15$ sections). The symbol ** represents $P < 0.01$ in comparison with control values.

Maternal cigarette smoke exposure compromises adult sperm production/function and decreases male fertility

Adult MSE animals had significantly reduced sperm counts (55% of control) and visual motility (67% of control) compared with control animals, supporting the histological evidence of reduced germ cell numbers and aberrant spermatogenesis (Fig. 10A and B). Sperm-zona pellucida binding assays revealed a significant decrease (50% of control) in the capacity of MSE spermatozoa to interact with the zona pellucida (Fig. 10C). Functional analysis of the spermatozoa's ability to undergo fertilization revealed an observable decrease in sperm-oocyte fusion in the MSE group compared with the control (56% of control), suggesting abnormal acrosome development (Fig. 10D).

MSE animals had a significant decrease in the percentage of morphologically normal spermatozoa compared with the control group, with a significant increase in head abnormalities (1.5-fold) and tail defects (3-fold) (Fig. 11A). Subsequent staining with FITC-PNA revealed both major and minor head defects in MSE spermatozoa were also characterized by severe acrosomal abnormalities or an absence of an acrosome altogether, although this may have been due to premature acrosome activation (Fig. 11B). The significant increase in tail defects matches the microarray data, with genes present in the spermatozoal flagellum being significantly down-regulated (Supplementary data, Table SV). One of these genes was the cytoskeletal axoneme protein *Odf2*. Immunocytological analysis localized Odf2 to both the acrosome and principle piece of morphologically normal sperm in control and smoke-exposed animals (Fig. 11C). Odf2 was localized to the midpiece of abnormal spermatozoa from the MSE group, with some spermatozoa also displaying sparse principle piece localization and an absence of Odf2 in the acrosome.

COMET analysis, an assay used to detect DNA damage in single cells, revealed a significant increase (~2-fold) in the number of spermatozoa with 'COMET heads' in adult MSE animals, suggesting a larger proportion of spermatozoa with significant DNA damage (Supplementary data, Fig. S5B). Further analysis also revealed a significant increase in Olive Tail Movement, an indicator of DNA damage severity, suggesting increased levels of DNA damage per spermatozoa in the adult MSE group (Supplementary data, Fig. S5C).

To confirm a decrease in the reproductive capacity of MSE males, we conducted a small scale fertility trial ($n = 5$ males) in 8-week-old adult offspring, concluding after 12 weeks cohabitation with females (Supplementary data, Fig. S6). Control males took on average 5 days to impregnate virgin females, as determined by post-coital plugs and date of littering. In contrast, adult MSE males took 9 days to impregnate virgin females, with one male failing to sire any litters (Supplementary data,

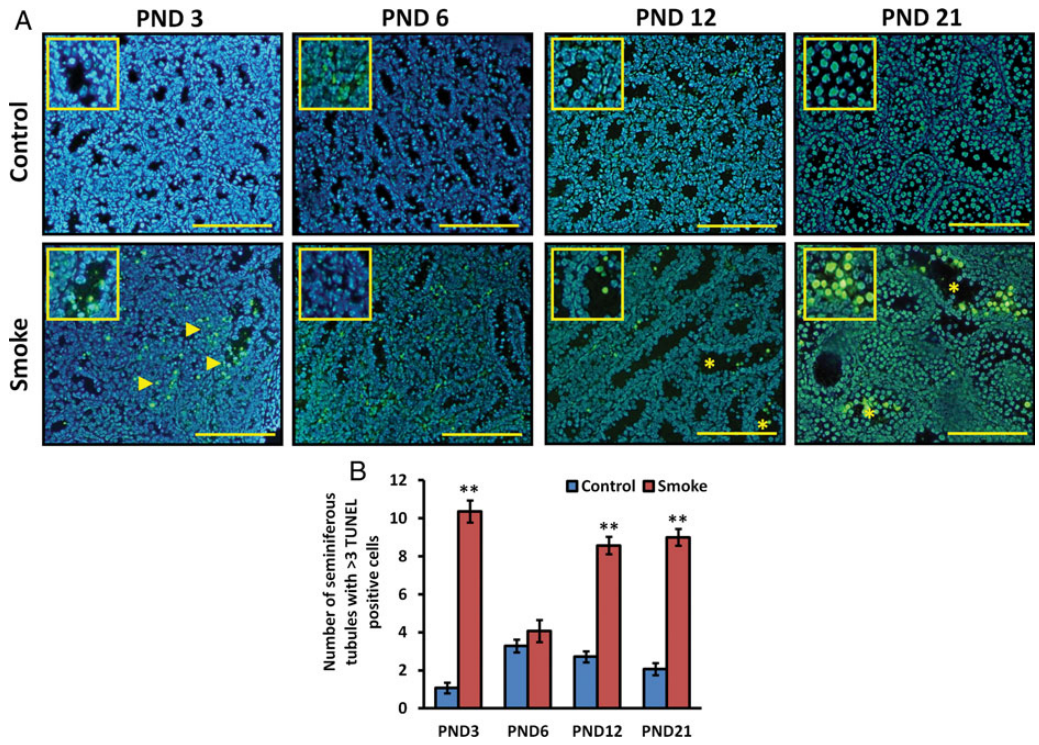

Figure 5 Maternal cigarette smoke exposure causes seminiferous tubule DNA damage in neonatal and juvenile offspring. (**A**) Fluorescent TUNEL staining (marker of DNA damage) visualized via epifluorescent microscopy. Images are representative of $n = 3$ experiments on $n = 3–5$ testes from individual mice belonging to different litters ($n = 9–15$ sections). Blue staining (DAPI) represents nuclear staining in all cells; green staining (Fluorescein) represents specific staining for degraded DNA (TUNEL). Arrow heads = cells with DNA damage; Asterisk = depleted tubules with DNA damaged cells. Scale bar is equal to 100 μm. (**B**) Quantification of the number of seminiferous tubules containing >3 TUNEL positive cells. Values are mean ± SEM, $n = 3$ experiments on $n = 3–5$ testes from individual mice belonging to different litters ($n = 9–15$ sections). The symbol ** represents $P < 0.01$ in comparison with control values.

Fig. S6A). There was also a slight but significant ($P < 0.01$) reduction in the average litter size of adult smoke-exposed males (Supplementary data, Fig. S6B).

Discussion

The present study was designed to examine the effects of MSE on male offspring reproduction by examining its effects on spermatogenesis, seminiferous tubule morphology, spermatozoal functionality and fertility. By making direct comparisons between two groups of mice from the same strain, control and exposed, we have controlled for other variables in a way which has not been possible in previous human studies. Our results demonstrate that maternal cigarette smoke exposure during the gestational/weaning period induces severe neonatal/juvenile germ cell depletion, manifesting as abnormal seminiferous tubule morphology in adulthood (Figs 1 and 2). The early depletion of these germ cells is apoptosis driven, supporting previous reports which implicate a similar mechanism in cigarette smoke-induced female germ cell loss (Figs 3–5) (Sobinoff *et al.*, 2011, 2012b,c, 2013; Sadeu and Foster, 2013). PND 3 testes contained germ cells at the most vulnerable time point, a period of development corresponding with gonocyte migration to the seminiferous tubule basement membrane (Itman *et al.*, 2006). This early depletion of gonocytes could negatively impact on the establishment of the spermatogonial stem cell pool, as evidenced by the lack of spermatogonia in maternal smoke-exposed juvenile/adult offspring (Fig. 6). Interestingly, there was only a slight increase in germ cell apoptosis at PND6, a time point which corresponds with the completed differentiation of gonocytes into spermatogonia (Itman *et al.*, 2006). This would suggest an increase in spermatogonial resistance to cigarette smoke-induced insult, a response which also occurs in neonatal ovarian primordial follicles exposed to cigarette smoke constituents (Sobinoff *et al.*, 2012b). Apoptosis was detected at PND12 and continued through to PND21, two time points corresponding to pachytene spermatocyte double strand break resolution and subsequent meiotic divisions (Itman *et al.*, 2006). Germ cells entering meiosis are particularly vulnerable to xenobiotic insult, resulting in improper chromosomal alignment and/or recombination (Zenzes, 2000). Indeed, we have previously shown that direct cigarette smoke exposure causes meiotic spindle disruption in meiosis II oocytes (Jennings *et al.*, 2011). Combined, these results suggest that early gonocytes and meiotic germ cells are vulnerable to maternal cigarette smoke exposure during weaning, with spermatogonial stem cells being resistant at PND6.

Unlike in neonatal and juvenile animals, both Casp2 and Casp3 were not detected above control levels in adult MSE testes, suggesting that the empty/disorganized seminiferous tubules observed at this time point were due to earlier pathology (Figs 2 and 7) and a result of loss of spermatogonial stem cells evidenced by reduced Sall4 and Plzf positive

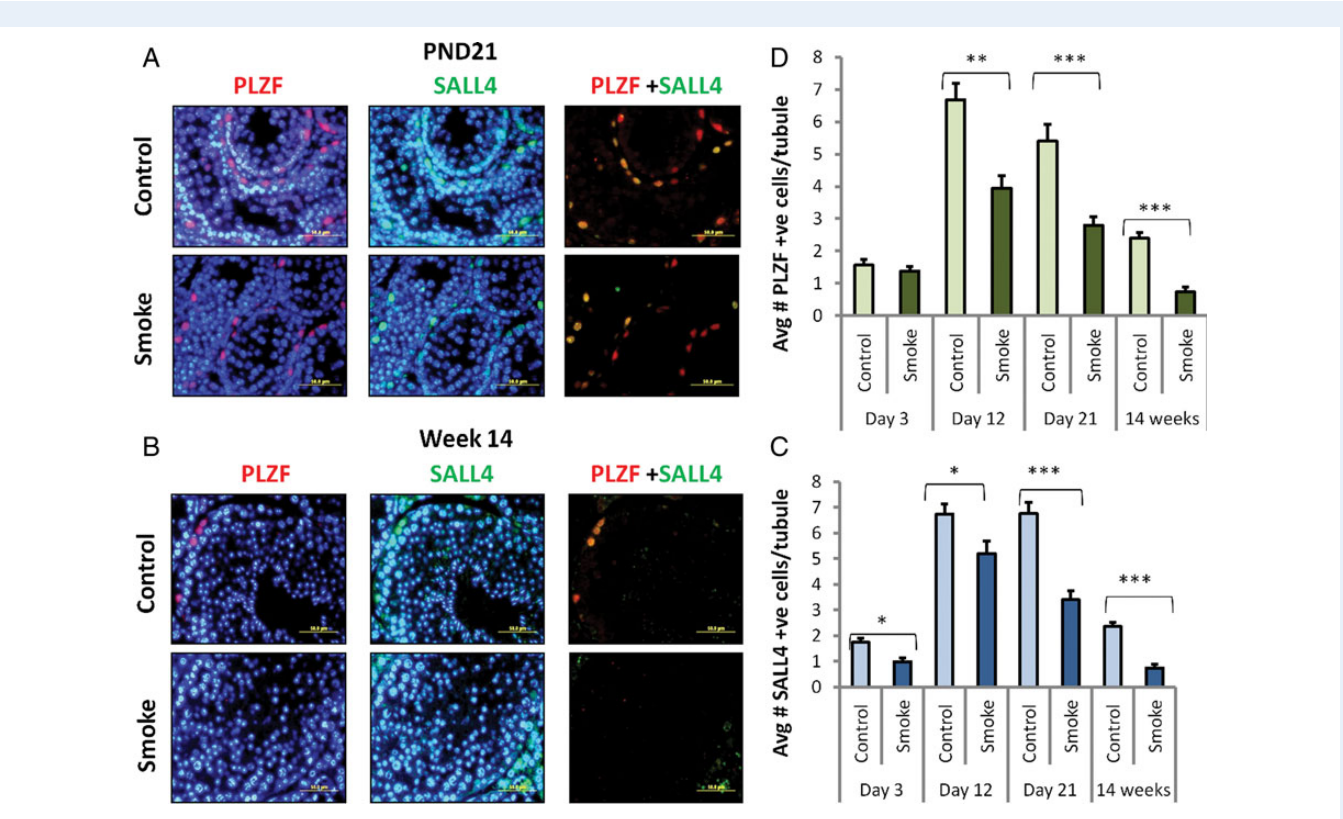

Figure 6 Maternal cigarette smoke exposure impairs the formation of the spermatogonial stem cell pool. (**A** and **B**) Fluorescent PLZF and SALL4 (markers of spermatogonial stem cells) immunohistological staining visualized via epifluorescent microscopy. Images are representative of $n = 3$ experiments on $n = 3–5$ testes from individual mice belonging to different litters ($n = 9–15$ sections). Blue staining (DAPI) represents nuclear staining in all cells; red staining (Cy-5) represents specific staining for PLZF protein; green staining (FITC) represents specific staining for SALL4 protein. (**C** and **D**) Average number of germ cells with PLZF or SALL4 immunolocalization. Values are mean ± SEM, $n = 50$ tubules from 3 to 4 individual testes from individual mice belonging to different litters; The symbols *, ** and *** represent $P < 0.05$, $P < 0.01$ and $P < 0.001$ compared with controls.

germ cells (Fig. 6) (Costoya *et al.*, 2004; Hobbs *et al.*, 2012). However, TUNEL staining revealed a significant increase in germ cell DNA damage, with PCNA and Dmc1 markers of DNA repair being localized in mitotic and meiotic germ cells, respectively (Fig. 8) (Chapman and Wolgemuth, 1994; Howard-Till *et al.*, 2011). The persistence of increased DNA damage in adult offspring suggests continued vulnerability due to long-term defects affecting spermatogenesis after maternal smoke exposure ceased. Indeed, neonatal exposure to cigarette smoke constituents causes long-term oocyte dysfunction due to increased oxidative stress originating from damaged mitochondria unable to repair due to long periods of quiescence (Sobinoff *et al.*, 2012a,c). Due to the high turnover of male germ cells and mitotic 'rejuvenation' during spermatogenesis, it is unlikely that a similar mechanism of toxicity is occurring in the male germ line (Kolasa *et al.*, 2012). However, microarray analysis of adult offspring did reveal an increase in glutathione metabolism signalling, a marker of increased oxidative stress. Canonical pathways analysis also revealed an increase in glycolysis, indicating a potential energy deficit due to inefficient mitochondrial metabolism (Warburg, 1956). In the context of increased oxidative stress, qPCR analysis identified the redox sensitive thioredoxin-interacting protein *Txnip* as up-regulated in smoke-exposed adults (Supplementary data, Table SV) (Sato *et al.*, 2008; Collet and Messens, 2010). Analysis of the mitochondrial genomes in MSE exposed males also revealed significant re-arrangements of the testicular mitochondrial genome, with almost twice the number of significant re-arrangements being observed when compared with lung tissue and unexposed testes (Supplementary data, Table SVI). The mitochondrial genome encodes 13 essential oxidative phosphorylation subunit proteins, two rRNAs (12S rRNA and 16S rRNA) and 22 tRNAs that are required for mitochondrial protein synthesis (Bibb *et al.*, 1981). The highest prevalence of testicular nucleotide re-arrangements occurred at segments encoding rRNA (nt2471 [91.98%] and nt2511 [51.72%]), the Nd4 subunit of Complex I (nt10818 [41.98%]) and the Cytb subunit of Complex III (nt14213 [74.14%]) (Supplementary data, Table SVII). These mutations could have significant consequences on mitochondrial function/energy production and oxidative stress, resulting in continued DNA damage long after MSE. Another potential cause of continued DNA damage may be the presence of DNA-macromolecular adducts. Many components of cigarette smoke are converted into highly reactive compounds through bioactivation, forming molecular adducts with DNA (Sobinoff *et al.*, 2012a). Interestingly, xenobiotic metabolism was demonstrated to be up-regulated in adult MSE offspring, suggesting the presence of potential adduct forming toxicants weeks after exposure.

Developing germ cells within the seminiferous epithelium are dependent on Sertoli 'nurse' cells for nutritional and structural support. Sertoli cell morphology in juvenile and adult MSE animals showed signs of dysfunction,

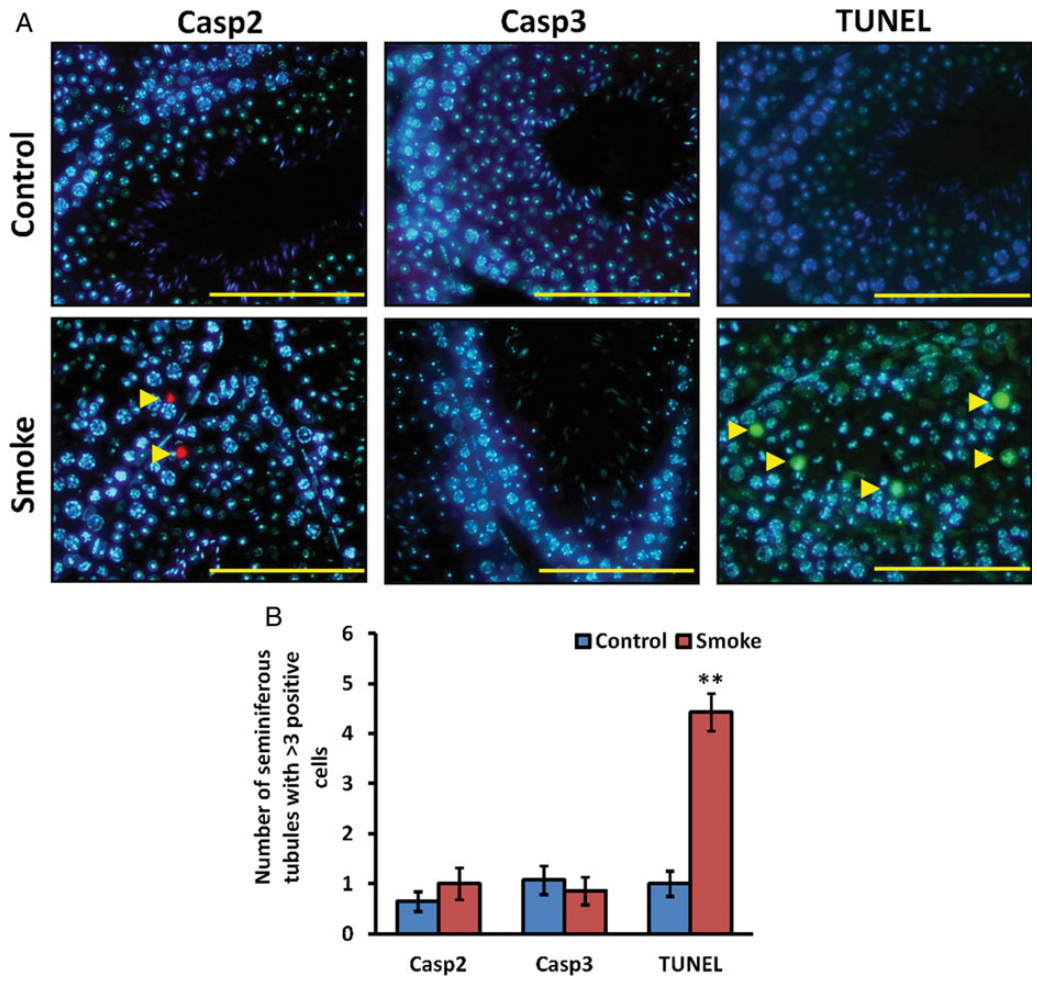

Figure 7 MSE offspring have increased levels of DNA damage without apoptosis in adulthood. (**A**) Fluorescent immunohistological and TUNEL staining visualized via epifluorescent microscopy. Images are representative of $n = 3$ experiments on $n = 3–4$ testes from individual mice belonging to different litters ($n = 9–15$ sections). Blue staining (DAPI) represents nuclear staining; red staining (Cy-5) represents specific staining for the protein of interest; green staining (Fluorescein) represents specific staining for DNA strand breaks (TUNEL). Arrow heads = cells with positive fluorescence. Scale bar is equal to 100 μm. (**B**) Average number of seminiferous tubules with containing >3 cells positive for Casp2, Casp3 and TUNEL staining. Values are mean ± SEM, $n = 3$ experiments on $n = 3–5$ testes from individual mice belonging to different litters ($n = 9–15$ sections). The symbol ** represents $P < 0.01$ in comparison with control values.

including increased vacuolization and the presence of Sertoli cell only tubules (Fig. 9). Microarray analysis also revealed changes in testicular tight junction signalling in smoke-exposed animals, a core component of Sertoli cell biology (Kopera *et al.*, 2010). QPCR analysis detected a significant increase in *Timp2* expression, a Sertoli cell matrix protein implicated in germ cell migration, tubule restructuring and apoptosis (Yao *et al.*, 2011). These morphological defects, combined with microarray data suggesting altered tight junction signalling, indicate impaired Sertoli cell function which most likely contributed to the aberrant seminiferous tubule morphology observed in MSE animals. Due to their non-proliferating nature, Sertoli cell damage and any consequent testes pathology could persist after exposure, resulting in the continued spermatogenic defects observed in adult exposed animals. Fowler and colleagues also recently described abnormal Sertoli cell desert hedgehog signalling in human male fetuses exposed *in utero*, suggesting the defects observed in MSE Sertoli cells begin during early fetal development (Fowler *et al.*, 2008).

Maternal cigarette smoke exposure also altered pathways intimately involved in spermatogenesis (Supplementary data, Fig. S4). Both retinol and glycolipid metabolism were perturbed in the smoke-exposed adult offspring, inhibition of the former preventing spermatogonial proliferation, and the latter impairing spermatogenesis (Van der Spoel *et al.*, 2002; Wolgemuth and Chung, 2007). In support of altered retinol signalling, qPCR analysis revealed an increase in *Retsat* expression, an enzyme responsible for the metabolism of vitamin A in the testes and a mediator of oxidative stress resistance (Nagaoka-Yasuda *et al.*, 2007; Schupp *et al.*, 2009). Maternal cigarette smoke exposure has also been shown to induce abnormal alveolarization through altered retinoic acid signalling in the lungs of offspring (Manoli *et al.*, 2012). Hormone metabolism was also found to be altered in exposed animals. The smoke constituent nicotine can interfere with hormone signalling via the hypothalamic-pituitary axis through the stimulation of growth hormone, cortisol and oxytocin release (Gyekis *et al.*, 2010). Given that hormone metabolism remained altered at

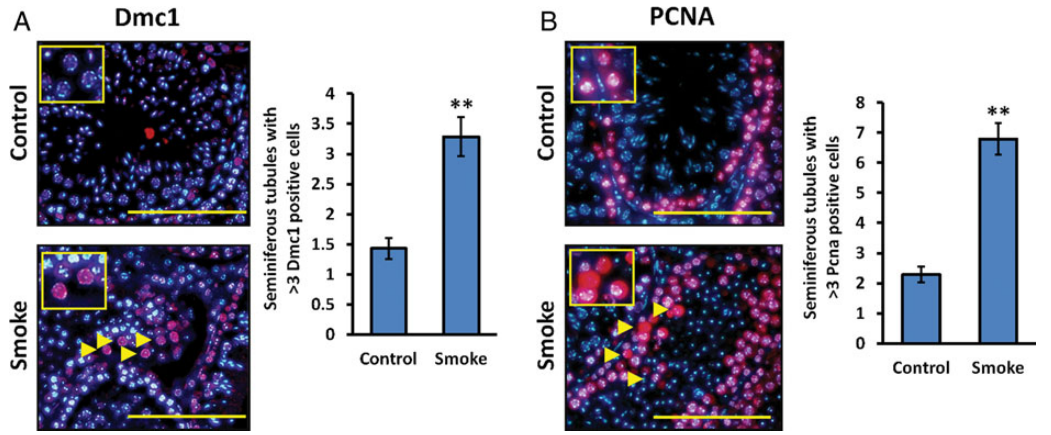

Figure 8 Fluorescent immunolocalization of Dmc1 (marker of meiotic DNA damage) (**A**) and PCNA (marker of proliferation and DNA damage) (**B**) in control and smoke-exposed testes. Representative image of both control and smoke-exposed testes (left panel) and average number of seminiferous tubules containing >3 positive cells (right panel). Blue staining (DAPI) represents nuclear staining in all cells; red staining (Cy-5) represents specific staining for the described protein. Values are mean ± SEM, $n = 3$ experiments on $n = 3$–4 testes from individual mice belonging to different litters ($n = 9$–12 sections); arrow head = positive cells highlighted in insert at higher magnification; scale bar is equal to 100 μm; the symbol ** represents $P < 0.01$ in comparison with control values.

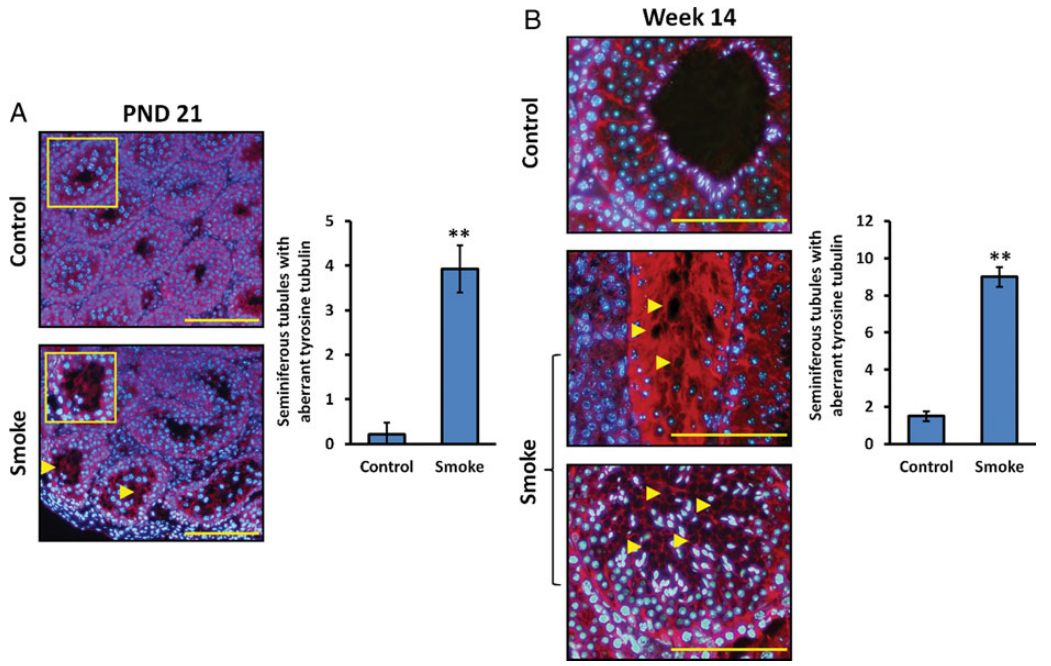

Figure 9 Maternal cigarette smoke exposure causes abnormal Sertoli cell morphology in juvenile and adult offspring. (**A**) Fluorescent immunolocalization of tyrosine tubulin (marker of Sertoli cells) in PND21 (A) and week 14 (**B**) in control and smoke-exposed testes. Representative image of both control and smoke-exposed testes (left panel) and the average number of seminiferous tubules with abnormal Sertoli cell staining (right panel). Blue staining (DAPI) represents nuclear staining in all cells; red staining (Cy-5) represents specific staining for tyrosine tubulin. The results presented here are representative of $n = 3$ experiments; Values are mean ± SEM, $n = 3$–4 testes from individual mice belonging to different litters ($n = 9$–12 sections); Arrow head = Sertoli cell vacuolization; scale bar is equal to 100 μm; the symbol ** represents $P < 0.01$ in comparison with control values.

11 weeks post weaning, we hypothesize that maternal smoke exposure, possibly through nicotine endocrine disruption, causes lasting effects on male offspring androgen action. QPCR analysis also revealed a significant increase in testicular *Cyp17a1* and *Cyp11a1* expression (Supplementary data, Table SV). Both of these cytochrome P450 enzymes play crucial roles in steroid biosynthetic pathways, including testosterone production

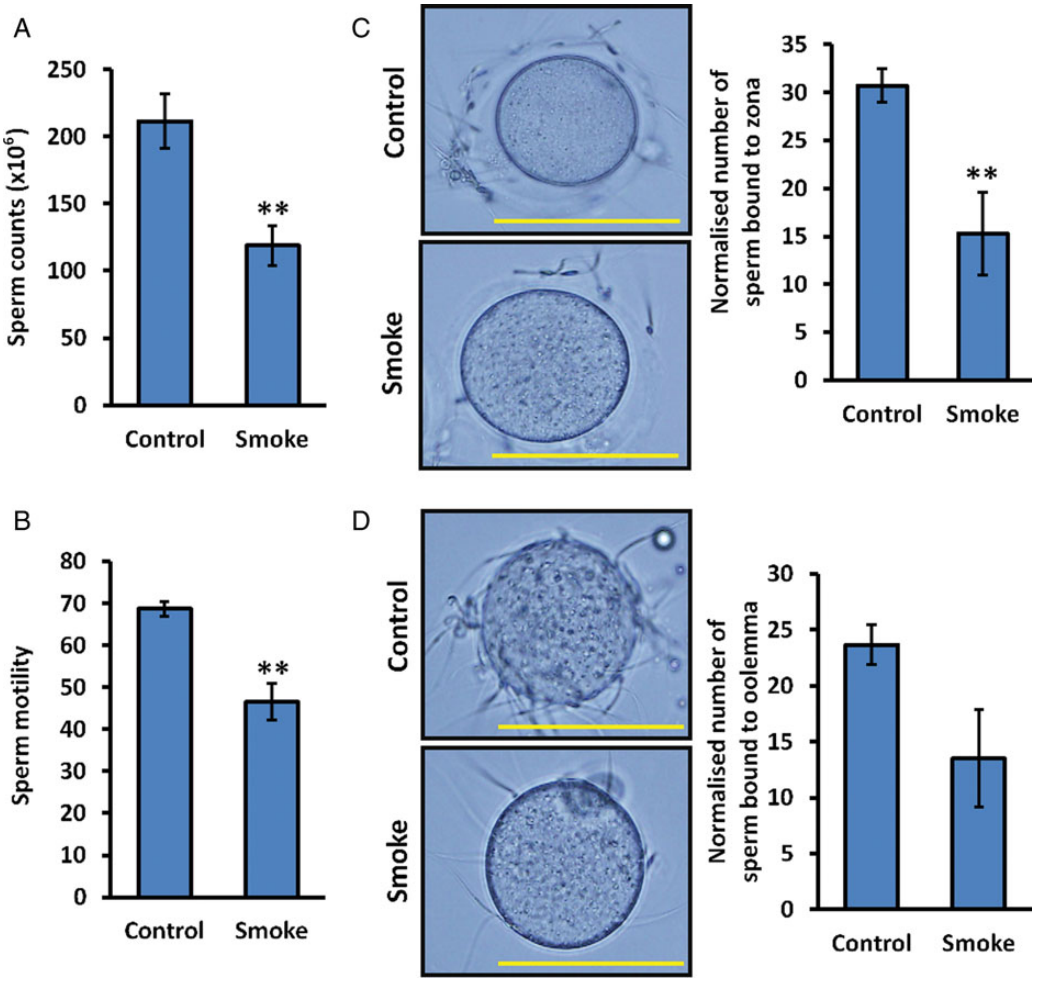

Figure 10 Maternal cigarette smoke exposure reduces adult offspring spermatozoa quantity and quality. (**A**) Average number of sperm extracted from the cauda epididymis. Results are normalized to uninfected control values. Values are mean ± SEM, $n = 3$ separate experiments on $n = 3$ individual mice belonging to different litters. The symbol ** represents $P < 0.01$ in comparison with control values. (**B**) Average sperm motility in each treatment group. Values are mean ± SEM, $n = 3$ separate experiments on $n = 3$ individual mice belonging to different litters. The symbol ** represents $P < 0.01$ in comparison with control values. Representative images of both control and smoke-exposed (**C**) zona-intact or (**D**) zona-free oocytes after sperm oocyte binding assays (left panel) and quantification of bound sperm after co-incubation (right panel). Results are representative of $n = 3$ experiments; values are mean ± SEM, $n = 12–25$ oocytes from six individual mice belonging to different litters; scale bar is equal to 100 μm; ** represents $P < 0.01$ compared with controls.

(Shan *et al.*, 1993). These enzymes are known to be vulnerable to chemical interference, with their increase in expression potentially affecting testosterone levels. Indeed, high levels of total serum testosterone have been detected in adult male smokers, although a persistent change after the cessation of smoking has not been reported (Trummer *et al.*, 2002).

In support of prolonged meiotic germ cell pathology in adult MSE animals, a number of genes expressed in spermatocytes and spermatids were significantly down-regulated (Supplementary data, Table SV). One of these genes was *Sycp1*, a synaptonemal complex protein involved in chromosome pairing and recombination during meiotic prophase (Meuwissen *et al.*, 1992). *Sycp1* knockout mice display normal spermatogenesis up until the spermatocyte stage, arresting in pachynema, diplonema and metaphase I (de Vries *et al.*, 2005). Another gene down-regulated in MSE testes was *Yxb2*, a germ cell-specific member of the Y-box family of DNA-/RNA-binding proteins (Gu *et al.*, 1998). *Ybx2* acts as a transcription cofactor for testis specific genes and is involved in RNA stabilization and storage following chromatin condensation (Giorgini *et al.*, 2001; Yang *et al.*, 2005a). Mice lacking *Ybx2* are infertile due to incomplete nuclear condensation, and fail to develop mature spermatozoa (Yang *et al.*, 2005b). Reduced *Sycp1* and *Ybx2* expression supports the observed reduction in the population of meiotic germ cells, and suggests abnormal meiotic recombination/nuclear condensation resulting in DNA damage and apoptosis (Figs 1, 7 and 10). *Acot7*, an acyl-CoA hydrolase expressed in spermatocytes and spermatids, was also down-regulated in maternal cigarette exposed adults (Supplementary data, Table SV) (Takagi *et al.*, 2006). Like *Sycp1* and *Ybx2*, a decrease in *Acot7* is indicative of a depleted spermatocyte population.

The pathological defects observed in adult testis histology translated to poor sperm counts and lower sperm motility and a decreased

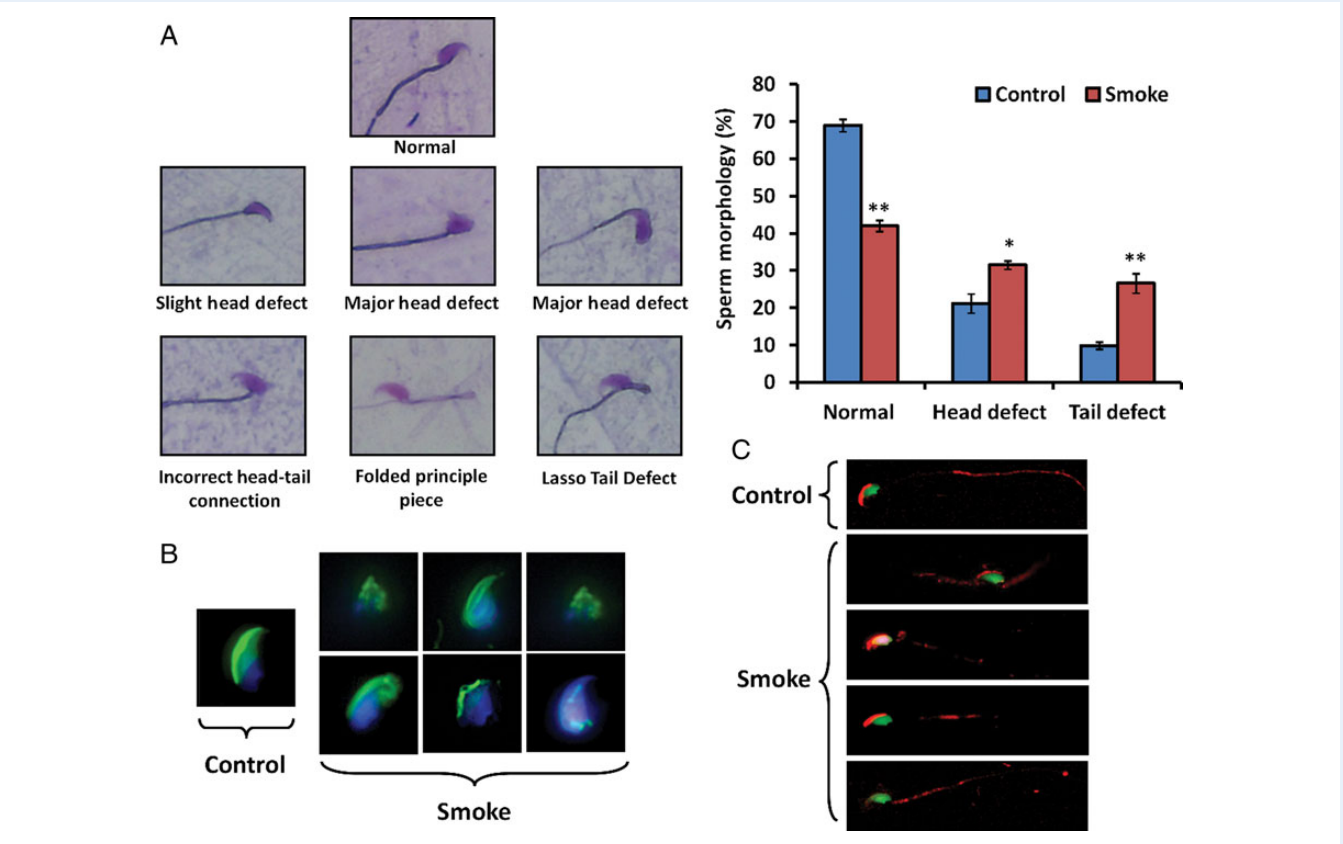

Figure 11 Effects of maternal cigarette smoke exposure on adult offspring spermatozoa morphology. (**A**) Representative images of abnormalities of spermatozoa morphology observed for each treatment (left panel) and quantification of spermatozoa with 'normal' morphology (right panel). Scale bar is equal to 5 μm. Results are expressed as a percentage. Values are mean ± SEM, $n = 3$ separate experiments on individual mice belonging to different litters. The symbols * and ** represent $P < 0.05$ and $P < 0.01$, respectively, in comparison with control values. (**B**) Representative images of acrosome morphology visualized with peanut agglutinin (acrosome marker). Blue staining (DAPI) represents nuclear staining in all cells; green staining (FITC) represents the acrosome. The results presented here are representative of $n = 3$ experiments on individual mice belonging to different litters. (**C**) Fluorescent immunolocalization of Odf2 in isolated spermatozoa. Green staining (YOYO®-1 Iodide) represents nuclear staining in all cells; red staining (Cy5) represents Odf2 localization.

ability to bind to the zona pellucida to initiate fertilization (Fig. 10). Although a significant number of spermatozoa had severe head defects with abnormal acrosome formation, the majority of defective spermatozoa displayed abnormal tail formation (Fig. 11A and B). Poor motility associated with abnormal tail development induced by smoke exposure may be attributed to the reduction in gene expression of *Akap4* and *Slc30a1*, both essential components of the sperm flagellum required for motility (Supplementary data, Table SV) (Miki *et al.*, 2002; Yamaguchi *et al.*, 2009). Reduction of the sperm flagellum component *Odf2* was also down-regulated in adult maternal cigarette exposed offspring (Supplementary data, Table SV) (Tarnasky *et al.*, 2010). Another study reported *Odf2* reduction in the lungs of human 'healthy' smokers, causing shortened airway cilia (Leopold *et al.*, 2009). Localization of Odf2 along the spermatozoa flagellum revealed abnormal localization in the midpiece in MSE offspring, with sparse principle piece localization (Fig. 11C). A hypomorph mouse model recently identified Odf2 as essential for basal foot formation, revealing a crucial role of this structure in the polarized alignment of basal bodies and coordinated ciliary beating (Kunimoto *et al.*, 2012). Therefore, a reduction in *Odf2* expression coupled with abnormal localization along the spermatozoa flagellum could impact motility by disrupting flagella movement. These spermatozoal defects most likely contributed to the increased time to conception and reduced litter sizes in adult MSE males (Supplementary data, Fig. S6).

The germ cell pathology observed in MSE offspring may also cause trans-generational toxicity. The increase in the number and severity of DNA damage in exposed spermatozoa revealed by COMET analysis has been associated with fertilization failure and potential damage to the fetus (Supplementary data, Fig. S6) (Simon *et al.*, 2011). Poor spermatozoal DNA integrity promotes the transmission of genetic aberrations to the conceptus, causing congenital malformations (Zini, 2011). In the context of tumorigenesis, the incidence of acute lymphoblastic leukaemia is significantly increased in patients with paternal smoke exposure around the time of conception, and is unrelated to maternal smoke exposure (Metayer *et al.*, 2013). Given the spermatozoa's limited ability to repair DNA damage, and that spermatozoa containing DNA lesions can still reach and fertilize an ovum, it has been hypothesized that the increase in oxidative/acid-induced DNA damage observed in male smokers could account for this increase in cancer susceptibility (Chandley,

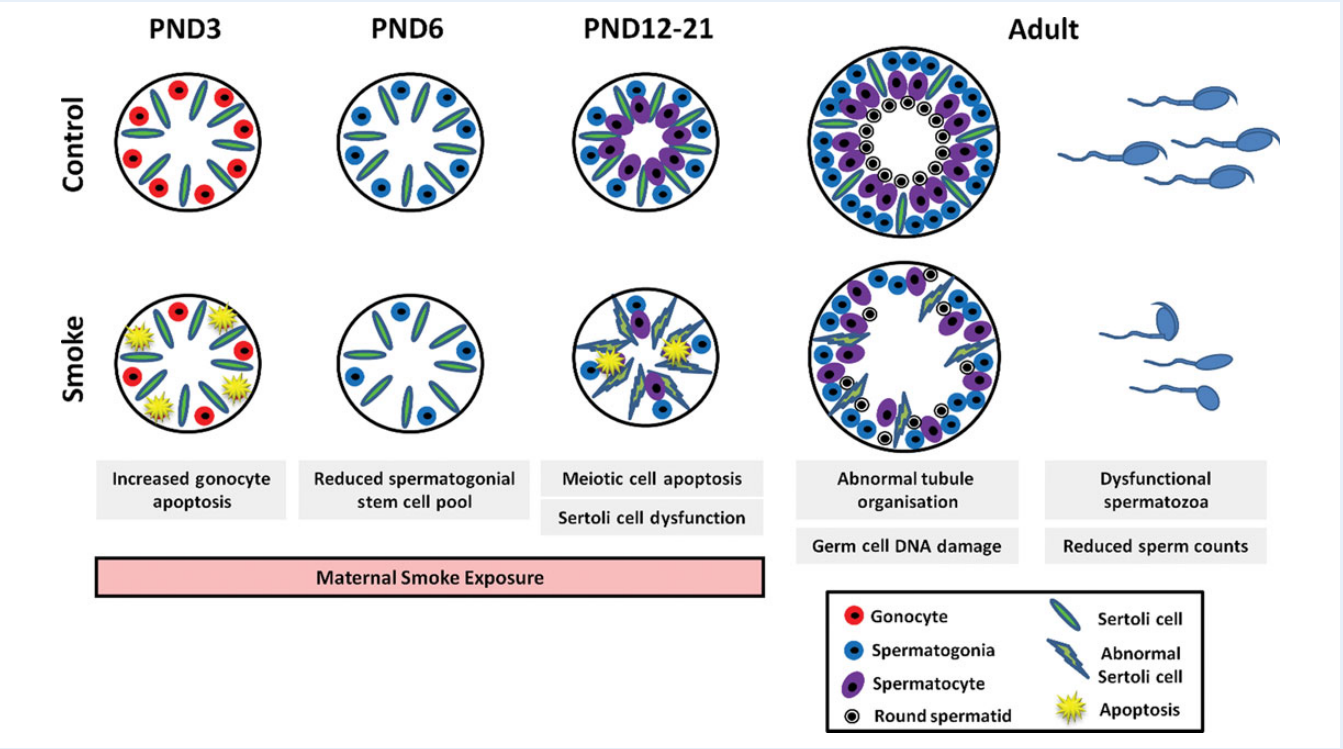

Figure 12 Graphical representation representing the effects of maternal smoke exposure on spermatogenesis in exposed offspring. Increased gonocyte apoptosis results in a decreased spermatogonial stem cell population. Continued MSE during weaning results in meiotic germ cell apoptosis and abnormal Sertoli cell formation, impairing seminiferous tubule organization and germ cell development. These defects cumulate in reduced sperm counts and abnormal spermatozoa morphology, impairing fertility.

1991; Fraga *et al.*, 1996; Sun *et al.*, 1997; Metayer *et al.*, 2013). The increase in spermatozoal DNA damage observed in MSE animals could contribute to increased cancer susceptibility in the F2 generation, despite the absence of direct cigarette smoke exposure in later life.

In conclusion, the findings of this study suggest that maternal cigarette smoke exposure during the gestational/weaning period results in the formation of a reduced spermatogonial stem cell population, impaired spermatogenic development and Sertoli cell dysfunction. This manifests in adulthood as reduced germ cell number, abnormal seminiferous tubule organization, germ cell DNA damage and defective spermatozoa (Fig. 12). This ultimately results in male factor subfertility and the potential for congenital malformations and cancer in F2 offspring, although we have not assayed for this. Future work should focus on the transgenerational effects of maternal cigarette exposure, including defects in fertility and increased cancer susceptibility in offspring and subsequent generations. This model could also be used to determine the effects of maternal smoking cessation at different stages of embryonic development and weaning on male offspring reproductive health. By controlling for external confounders present in human epidemiological studies, this report provides strong evidence useful for informing the public about the consequences of female smoking on the health of male offspring, facilitating quit smoking campaigns for pregnant and lactating women.

Supplementary data

Supplementary data are available at http://humrep.oxfordjournals.org/.

Acknowledgements

The authors are grateful for advice given by Assoc Prof Brett Nixon and Dr Shaun Roman.

Authors' roles

A.P.S. contributed to the conception and design of the study, the acquisition of data and the analysis/interpretation of data. He was also responsible for drafting and revising the manuscript. J.M.S., E.L.B., S.J.S., R.J., A.G.J. and J.C.S. contributed to data acquisition. J.M.S., S.J.S., and J.C.S. contributed to the analysis/interpretation of the data. A.M., J.C.S., P.M.H. and E.A.M. contributed to the conception and design of the study. All authors reviewed and approved the final manuscript. E.A.M. is the guarantor and takes full responsibility for the work as a whole.

Funding

The authors gratefully acknowledge the financial assistance to E.A.M. and P.M.H. by the Australian Research Council, Hunter Medical Research Institute, National Health and Medical Research Council of Australia and the Newcastle Permanent Building Society Charitable Trust (HMRI 06-34). J.C.S.J was supported by the Victorian Government's Operational Infrastructure Support Program.

Conflict of interest

The authors declare no conflict of interest.

References

AIFS. The Longitudinal Study of Australian Children Annual statistical report 2010. In: Hayes A (ed). *Growing up in Australia: The Longitudinal Study of Australian Children (LSAC)*. Australian Institute of Family Studies, 132. (2011).

Andres RL, Day MC. Perinatal complications associated with maternal tobacco use. *Semin Neonatol* 2000;**5**:231–241.

Beckett EL, Stevens RL, Jarnicki AG, Kim RY, Hanish I, Hansbro NG, Deane A, Keely S, Horvat JC, Yang M *et al.* A short-term model of COPD identifies a role for mast cell tryptase. *J Allergy Clin Immunol* 2013; **131**:752–762.

Belcheva A, Ivanova-Kicheva M, Tzvetkova P, Marinov M. Effects of cigarette smoking on sperm plasma membrane integrity and DNA fragmentation. *Int J Androl* 2004;**27**:296–300.

Bibb MJ, Van Etten RA, Wright CT, Walberg MW, Clayton DA. Sequence and gene organisation of mouse mitochondrial DNA. *Cell* 1981; **26**:167–180.

Carmichael SL, Shaw GM, Laurent C, Lammer EJ, Olney RS. Hypospadias and maternal exposures to cigarette smoke. *Paediatr Perinat Epidemiol* 2005; **19**:406–412.

CDC. *Pregnancy Risk Assessment Monitoring System (PRAMS) and Smoking Data Tables, Vol. 2013*. Centers for Disease Control and Prevention (2011).

Chandley AC. On the parental origin of *de novo* mutation in man. *J Med Genet* 1991;**28**:217–223.

Chapman DL, Wolgemuth DJ. Expression of proliferating cell nuclear antigen in the mouse germ line and surrounding somatic cells suggests both proliferation-dependent and -independent modes of function. *Int J Dev Biol* 1994;**38**:491–497.

Chomczynski P, Sacchi N. Single-step method of RNA isolation by acid guanidinium thiocyanate-phenol-chloroform. *Anal Biochem* 1987; **162**:156–159.

Collet JF, Messens J. Structure, function, and mechanism of thioredoxin proteins. *Antioxid Redox Signal* 2010;**13**:1205–1216.

Costoya JA, Hobbs RM, Barna M, Cattoretti G, Manova K, Sukhwani M, Orwig KE, Wolgemuth DJ, Pandolfi PP. Essential role of Plzf in maintenance of spermatogonial stem cells. *Nat Genet* 2004;**36**:653–659.

Damgaard IN, Jensen TK, Petersen JH, Skakkebaek NE, Toppari J, Main KM. Risk factors for congenital cryptorchidism in a prospective birth cohort study. *PLoS One* 2008;**3**:e3051.

de Vries FA, de Boer E, van den Bosch M, Baarends WM, Ooms M, Yuan L, Liu JG, van Zeeland AA, Heyting C, Pastink A. Mouse Sycp1 functions in synaptonemal complex assembly, meiotic recombination, and XY body formation. *Genes Dev* 2005;**19**:1376–1389.

Fowler PA, Cassie S, Rhind SM, Brewer MJ, Collinson JM, Lea RG, Baker PJ, Bhattacharya S, O'Shaughnessy PJ. Maternal smoking during pregnancy specifically reduces human fetal desert hedgehog gene expression during testis development. *J Clin Endocrinol Metab* 2008;**93**:619–626.

Fraga CG, Motchnik PA, Wyrobek AJ, Rempel DM, Ames BN. Smoking and low antioxidant levels increase oxidative damage to sperm DNA. *Mutat Res* 1996;**351**:199–203.

Giorgini F, Davies HG, Braun RE. MSY2 and MSY4 bind a conserved sequence in the 3′ untranslated region of protamine 1 mRNA *in vitro* and *in vivo*. *Mol Cell Biol* 2001;**21**:7010–7019.

Gu W, Tekur S, Reinbold R, Eppig JJ, Choi YC, Zheng JZ, Murray MT, Hecht NB. Mammalian male and female germ cells express a germ cell-specific Y-Box protein, MSY2. *Biol Reprod* 1998;**59**:1266–1274.

Gyekis J, Anthony K, Foreman JE, Klein LC, Vandenbergh DJ. Perinatal nicotine exposure delays genital development in mice. *Reprod Toxicol* 2010;**29**:378–380.

Habek D, Habek JC, Ivanisević M, Djelmis J. Fetal tobacco syndrome and perinatal outcome. *Fetal Diagn Ther* 2002;**17**:367–371.

Hobbs RM, Fagoonee S, Papa A, Webster K, Altruda F, Nishinakamura R, Chai L, Pandolfi PP. Functional antagonism between Sall4 and Plzf defines germline progenitors. *Cell Stem Cell* 2012;**10**:284–298.

Howard-Till RA, Lukaszewicz A, Loidl J. The recombinases Rad51 and Dmc1 play distinct roles in DNA break repair and recombination partner choice in the meiosis of Tetrahymena. *PLoS Genet* 2011;**7**:e1001359.

Itman C, Mendis S, Barakat B, Loveland KL. All in the family: TGF-beta family action in testis development. *Reproduction* 2006;**132**:233–246.

Jennings PC, Merriman JA, Beckett EL, Hansbro PM, Jones KT. Increased zona pellucida thickness and meiotic spindle disruption in oocytes from cigarette smoking mice. *Hum Reprod* 2011;**26**:878–884.

Jensen TK, Jørgensen N, Punab M, Haugen TB, Suominen J, Zilaitiene B, Horte A, Andersen AG, Carlsen E, Magnus Ø *et al.* Association of in utero exposure to maternal smoking with reduced semen quality and testis size in adulthood: a cross-sectional study of 1,770 young men from the general population in five European countries. *Am J Epidemiol* 2004; **159**:49–58.

Kolasa A, Misiakiewicz K, Marchlewicz M, Wiszniewska B. The generation of spermatogonial stem cells and spermatogonia in mammals. *Reprod Biol* 2012;**12**:5–23.

Kopera IA, Bilinska B, Cheng CY, Mruk DD. Sertoli-germ cell junctions in the testis: a review of recent data. *Philos Trans R Soc Lond B Biol Sci* 2010; **365**:1593–1605.

Kunimoto K, Yamazaki Y, Nishida T, Shinohara K, Ishikawa H, Hasegawa T, Okanoue T, Hamada H, Noda T, Tamura A *et al.* Coordinated ciliary beating requires Odf2-mediated polarization of basal bodies via basal feet. *Cell* 2012;**148**:189–200.

Leopold PL, O'Mahony MJ, Lian XJ, Tilley AE, Harvey BG, Crystal RG. Smoking is associated with shortened airway cilia. *PLoS One* 2009;**4**:e8157.

Mamsen LS, Lutterodt MC, Andersen EW, Skouby SO, Sørensen KP, Andersen CY, Byskov AG. Cigarette smoking during early pregnancy reduces the number of embryonic germ and somatic cells. *Hum Reprod* 2010;**25**:2755–2761.

Manoli SE, Smith LA, Vyhlidal CA, An CH, Porrata Y, Cardoso WV, Baron RM, Haley KJ. Maternal smoking and the retinoid pathway in the developing lung. *Respir Res* 2012;**13**:42.

Metayer C, Zhang L, Wiemels JL, Bartley K, Schiffman J, Ma X, Aldrich MC, Chang JS, Selvin S, Fu CH *et al.* Tobacco smoke exposure and the risk of childhood acute lymphoblastic and myeloid leukemias by cytogenetic subtype. *Cancer Epidemiol Biomarkers Prev* 2013;**22**:1600–1611.

Meuwissen RL, Offenberg HH, Dietrich AJ, Riesewijk A, van Iersel M, Heyting C. A coiled-coil related protein specific for synapsed regions of meiotic prophase chromosomes. *EMBO J* 1992;**11**:5091–5100.

Miki K, Willis WD, Brown PR, Goulding EH, Fulcher KD, Eddy EM. Targeted disruption of the Akap4 gene causes defects in sperm flagellum and motility. *Dev Biol* 2002;**248**:331–342.

Møller H, Skakkebaek NE. Testicular cancer and cryptorchidism in relation to prenatal factors: case-control studies in Denmark. *Cancer Causes Control* 1997;**8**:904–912.

Nagaoka-Yasuda R, Matsuo N, Perkins B, Limbaeck-Stokin K, Mayford M. An RNAi-based genetic screen for oxidative stress resistance reveals retinol saturase as a mediator of stress resistance. *Free Radic Biol Med* 2007;**43**:781–788.

Rogers JM. Tobacco and pregnancy: overview of exposures and effects. *Birth Defects Res C Embryo Today* 2008;**84**:1–15.

Russell RW. Essential roles for animal models in understanding human toxicities. *Neurosci Biobehav Rev* 1991;**15**:7–11.

Sadeu JC, Foster WG. The cigarette smoke constituent benzo[a]pyrene disrupts metabolic enzyme, and apoptosis pathway member gene expression in ovarian follicles. *Reprod Toxicol* 2013;**40**:52–59.

Sato A, Hoshino Y, Hara T, Muro S, Nakamura H, Mishima M, Yodoi J. Thioredoxin-1 ameliorates cigarette smoke-induced lung inflammation and emphysema in mice. *J Pharmacol Exp Ther* 2008;**325**:380–388.

Schupp M, Lefterova MI, Janke J, Leitner K, Cristancho AG, Mullican SE, Qatanani M, Szwergold N, Steger DJ, Curtin JC *et al.* Retinol saturase promotes adipogenesis and is downregulated in obesity. *Proc Natl Acad Sci USA* 2009;**106**:1105–1110.

Shan LX, Phillips DM, Bardin CW, Hardy MP. Differential regulation of steroidogenic enzymes during differentiation optimizes testosterone production by adult rat Leydig cells. *Endocrinology* 1993;**133**:2277–2283.

Simon L, Lutton D, McManus J, Lewis SE. Sperm DNA damage measured by the alkaline Comet assay as an independent predictor of male infertility and *in vitro* fertilization success. *Fertil Steril* 2011;**95**:652–657.

Sobinoff AP, Pye V, Nixon B, Roman SD, McLaughlin EA. Adding insult to injury: effects of xenobiotic-induced preantral ovotoxicity on ovarian development and oocyte fusibility. *Toxicol Sci* 2010;**118**:653–666.

Sobinoff AP, Mahony M, Nixon B, Roman SD, McLaughlin EA. Understanding the Villain: DMBA-induced preantral ovotoxicity involves selective follicular destruction and primordial follicle activation through PI3K/Akt and mTOR signaling. *Toxicol Sci* 2011;**123**:563–575.

Sobinoff AP, Bernstein IR, McLaughlin EA. All your eggs in one basket; mechanisms of xenobiotic induced female reproductive senescence. *Senescence* 2012a;559–584.

Sobinoff AP, Nixon B, Roman SD, McLaughlin EA. Staying alive: PI3K pathway promotes primordial follicle activation and survival in response to 3MC-induced ovotoxicity. *Toxicol Sci* 2012b;**128**:258–271.

Sobinoff AP, Pye V, Nixon B, Roman SD, McLaughlin EA. Jumping the gun: smoking constituent BaP causes premature primordial follicle activation and impairs oocyte fusibility through oxidative stress. *Toxicol Appl Pharmacol* 2012c;**260**:70–80.

Sobinoff AP, Beckett EL, Jarnicki AG, Sutherland JM, McCluskey A, Hansbro PM, McLaughlin EA. Scrambled and fried: Cigarette smoke exposure causes antral follicle destruction and oocyte dysfunction through oxidative stress. *Toxicol Appl Pharmacol* 2013;**271**:156–167.

Storgaard L, Bonde JP, Ernst E, Spanô M, Andersen CY, Frydenberg M, Olsen J. Does smoking during pregnancy affect sons' sperm counts? *Epidemiology* 2003;**14**:278–286.

Sun JG, Jurisicova A, Casper RF. Detection of deoxyribonucleic acid fragmentation in human sperm: correlation with fertilization *in vitro*. *Biol Reprod* 1997;**56**:602–607.

Takagi M, Ohtomo T, Hiratsuka K, Kuramochi Y, Suga T, Yamada J. Localization of a long-chain acyl-CoA hydrolase in spermatogenic cells in mice. *Arch Biochem Biophys* 2006;**446**:161–166.

Tarnasky H, Cheng M, Ou Y, Thundathil JC, Oko R, van der Hoorn FA. Gene trap mutation of murine outer dense fiber protein-2 gene can result in sperm tail abnormalities in mice with high percentage chimaerism. *BMC Dev Biol* 2010;**10**:67.

Trummer H, Habermann H, Haas J, Pummer K. The impact of cigarette smoking on human semen parameters and hormones. *Hum Reprod* 2002;**17**:1554–1559.

Van der Spoel AC, Jeyakumar M, Butters TD, Charlton HM, Moore HD, Dwek RA, Platt FM. Reversible infertility in male mice after oral administration of alkylated imino sugars: a nonhormonal approach to male contraception. *Proc Natl Acad Sci USA* 2002;**99**:17173–17178.

Warburg O. On the origin of cancer cells. *Science* 1956;**123**:309–314.

Wolgemuth DJ, Chung SS. Retinoid signaling during spermatogenesis as revealed by genetic and metabolic manipulations of retinoic acid receptor alpha. *Soc Reprod Fertil Suppl* 2007;**63**:11–23.

Yamaguchi S, Miura C, Kikuchi K, Celino FT, Agusa T, Tanabe S, Miura T. Zinc is an essential trace element for spermatogenesis. *Proc Natl Acad Sci USA* 2009;**106**:10859–10864.

Yang J, Medvedev S, Reddi PP, Schultz RM, Hecht NB. The DNA/RNA-binding protein MSY2 marks specific transcripts for cytoplasmic storage in mouse male germ cells. *Proc Natl Acad Sci USA* 2005a;**102**:1513–1518.

Yang J, Medvedev S, Yu J, Tang LC, Agno JE, Matzuk MM, Schultz RM, Hecht NB. Absence of the DNA-/RNA-binding protein MSY2 results in male and female infertility. *Proc Natl Acad Sci USA* 2005b;**102**:5755–5760.

Yao PL, Lin YC, Richburg JH. Transcriptional suppression of Sertoli cell Timp2 in rodents following mono-(2-ethylhexyl) phthalate exposure is regulated by CEBPA and MYC. *Biol Reprod* 2011;**85**:1203–1215.

Zenzes MT. Smoking and reproduction: gene damage to human gametes and embryos. *Hum Reprod Update* 2000;**6**:122–131.

Zini A. Are sperm chromatin and DNA defects relevant in the clinic? *Syst Biol Reprod Med* 2011;**57**:78–85.